Reviewed Preprint
v1 • September 26, 2025
Not revised

Reviewed Preprint
v2 • August 10, 2026
Revised by authors

For correspondence:
sjm20@cam.ac.uk

* contributed equally

Competing interests: No competing interests declared

Funding: See page 29

Reviewing editor: Julien Roche, Iowa State University, United States

A GCN1-independent activator of the kinase GCN2

JiaYi Zhu[1,*], Giulia Emanuelli[1,*], Glenn R Masson[2], Vanesa Vinciauskaite[2], Henriette Willems[3], Peiqiao Cai[1], Andrew Lim[3], Christopher Alan Brown[3], David Winpenny[3], Murray Clarke[4], Rebecca Gilley[5], Fergus Preston[6], Jordan CJ Wilson[7], Aldo Bader[7], Taufiq Rahman[8], Joseph E Chambers[1], John Skidmore[3], Nicholas W Morrell[4,9], Stefan J Marciniak[1,4,9]

[1]Cambridge Institute for Medical Research (CIMR), University of Cambridge, Cambridge, United Kingdom • [2]Division of Cancer Research, School of Medicine, Ninewells Hospital, Dundee, United Kingdom • [3]The ALBORADA Drug Discovery Institute, University of Cambridge, Cambridge, United Kingdom • [4]Department of Medicine, University of Cambridge, Cambridge, United Kingdom • [5]Signalling Programme, The Babraham Institute, Babraham Research Campus, Cambridge, United Kingdom • [6]Domainex Ltd, Saffron Walden, United Kingdom • [7]Cancer Research UK Cambridge Institute, University of Cambridge, Cambridge, United Kingdom • [8]Department of Pharmacology, University of Cambridge, Cambridge, United Kingdom • [9]Royal Papworth Hospital NHS Foundation Trust, Cambridge, United Kingdom

eLife Assessment

This **important** study presents a cell-based screen for small-molecule activators of GCN2, an eIF2α kinase that regulates the Integrated Stress Response under diverse stress conditions. The authors identify a compound as a potent GCN2 activator with GCN1-independent activity under the tested conditions, providing a new pharmacological tool for probing GCN2 regulation. The revised manuscript provides **compelling** support for the central conclusions through a clearer description of the screening workflow, extended kinetic analyses, and demonstration that the identified compound causes a GCN2-dependent reduction in protein synthesis.

https://doi.org/10.7554/eLife.108590.2.sa4

Abstract

Mutations of *EIF2AK4*, which encodes the eIF2α kinase GCN2, cause a severe inherited form of pulmonary hypertension called pulmonary veno-occlusive disease (PVOD). Some pathogenic variants of GCN2 are amenable to pharmacological reactivation by low concentrations of ATP-pocket binding inhibitors. Kinase inhibition at modestly elevated concentrations limits the clinical utility of these drugs against PVOD. We therefore performed an *in cellulo* chemical screen for GCN2 activators and identified three structurally distinct compounds with low micromolar stimulatory activities. Unlike previously described GCN2 activators, one of these molecules activated GCN2 independently of GCN1. Modelling supported by structure activity screens suggested it binds within the ATP-pocket of GCN2, but unlike existing ligands does not protrude inward into the allosteric pocket or outward into the solvent. This overcomes a key requirement of other GCN2 activators.

Introduction

Phosphorylation of eukaryotic translation initiation factor 2 alpha (eIF2α) mediates the response to a variety of stresses by regulating translation, metabolism and cell survival (1, 2). In yeast, GCN2 is the sole eIF2α kinase and triggers the General Control Response to the accumulation of uncharged tRNA and to ribosome stalling (3, 4). Gene duplication gave rise to a family of eIF2α

kinases in multicellular organisms linking eIF2α phosphorylation to a variety of other stresses. HRI (EIF2AK1) is activated by haem deficiency, oxidative stress and mitochondrial dysfunction (5–7), PKR (EIF2AK2) responds to cytosolic double stranded RNA during viral infections, while PERK (EIF2AK3) is activated by endoplasmic reticulum (ER) stress (2). Mutations affecting these kinases have been linked to the development of disease and so their manipulation by small molecules is being pursued as a means to develop therapies (2, 8–11).

The eIF2 complex recruits initiator methionyl-tRNA to ribosomes commencing protein synthesis (2). This requires eIF2 to bind GTP, which is subsequently hydrolysed. Bound GTP is replenished by the guanine nucleotide exchange factor (GEF) eIF2B (12), but phosphorylated p-eIF2α binds avidly to eIF2B inhibiting its GEF activity (13). When levels of eIF2-GTP-tRNA-Met subsequently fall, most translation is disfavoured, but some transcripts are translated more efficiently owing to the presence of upstream open reading frames (uORFs) within their 5' untranslated regions (5'UTRs) (1, 14). ATF4 and CHOP are transcription factors upregulated in this manner during stress to induce genes of the Integrated Stress Response (ISR) (1, 2, 14). Eventually, PPP1R15A (also called GADD34), itself an ISR target, dephosphorylates p-eIF2α to restore the basal state (15, 16).

GCN2 is comprised of five domains—RWD, pseudokinase, kinase, HisRS-like, and C-terminal—and exists constitutively as a homodimer (17, 18). Its kinase activity is stimulated when the RWD domain interacts with colliding ribosomes via the cofactor GCN1 (19–21) or when the HisRS domain interacts with deacylated tRNAs (22, 23). Direct interaction between GCN2 and the ribosome P-stalk can also mediate GCN2 activation during ribosome stalling (24, 25).

Mutations of *EIF2AK4*, which encodes GCN2, cause the aggressive subtypes of familial pulmonary hypertension, pulmonary veno-occlusive disease (PVOD) and pulmonary capillary haemangiomatosis (PCH) (2, 17). Some pathogenic alleles generate hypomorphic variants of GCN2 that we and others have shown can be activated by small molecule inhibitors that bind to the GCN2 ATP pocket, e.g. neratinib and GCN2iB (9, 11, 26). Type 1 inhibitors bind the ATP pocket of the kinase in its active conformation (DFG-Asp-in, αC-helix-in), while type 2 inhibitors bind the inactive conformation (DFG-out, αC-helix-out) (27). Type 1.5 inhibitors, by contrast, bind an intermediate conformation (DFG-Asp-in, αC-helix-out). Several kinase inhibitors classified as type 1 or type 1.5 with respect to their canonical targets can activate GCN2 at low concentrations while inhibiting it at higher concentrations; however, their binding mode to GCN2 remains undefined (9, 11, 26). GCN2iB is a relatively selective type 1.5 inhibitor of GCN2 that activates the kinase at submicromolar concentrations (9, 17). It is hypothesised that drug-induced stabilisation of one GCN2 protomer within a dimer is propagated to the second protomer to cause its activation (11, 28). Several inhibitors of other kinases that are in clinical use or development as anticancer agents activate GCN2 in a GCN1-dependent manner, which may contribute to their therapeutic efficacy (26, 29–31). For this reason, GCN2 activators are being sought as potential anticancer drugs.

The complexity of GCN2 activation, involving direct and indirect detection of amino acid deprivation and ribosome stalling, has hampered efforts to reconstitute GCN2 function *in vitro* (32–34). We therefore performed a cell-based chemical screen for GCN2-dependent activators of the ISR, followed by *in vitro* validation using orthogonal approaches. In doing so, we identified three novel, structurally distinct GCN2 activators. Notably, one of these, designated compound 20, activates GCN2 in a GCN1-independent manner.

Results

Chemical screen for GCN2 activators

We generated clonal Chinese Hamster Ovary (CHO) cell lines expressing an ATF4::NanoLuc reporter comprising the 5' untranslated region (UTR) of human ATF4 mRNA fused to NanoLuc luciferase (Figure 1A) (17). Activation of the ISR could be detected as bioluminescence in response to ISR activators histidinol, tunicamycin and latrunculin A (Figure 1B). Histidinol activates GCN2 by inhibiting histidyl-tRNA synthetase, leading to the accumulation of uncharged $tRNA^{His}$. This uncharged tRNA binds to GCN2, relieving its autoinhibition and activating the kinase (35). Latrunculin A sequesters G-actin, thereby inhibiting PPP1R15A activity (36, 37). Tunicamycin

inhibits protein glycosylation in the endoplasmic reticulum (ER), resulting in activation of PERK (38). A high-throughput screen of the BioAscent library of 123,222 drug-like compounds performed by the ALBORADA Drug Discovery Institute yielded two pools of potential ISR inhibitors and activators. Compounds were classified based on Z-score thresholds derived from the primary screen, with activators defined as those with Z-score > 3. An initial analysis of 121,000 compounds, excluding plates failing quality control, identified 6,521 activators, of which 6,461 overlapped with the subset selected for follow-up screening. Minor discrepancies were restricted to compounds absent from the analysed dataset (e.g. originating from failed plates) or those with Z-scores close to the threshold (3 to 3.02), consistent with limited analytical variation. Using this approach, we assembled a subset of 6,461 compounds enriched for potential ISR activators and screened these in 384-well format at 10μM for 16 hours. To increase sensitivity, screens were performed with test compound alone or combined with the half-maximal effective concentration (EC_{50}) of histidinol. This submaximal concentration was used to allow detection of compounds that enhance ISR signalling when GCN2 is partially activated. This yielded 153 compounds that activated the reporter at least three standard deviations above baseline (Z-score > 3) (Figure 1C).

The pipeline used to filter hit compounds is illustrated in Figure 1D. Counter screens were performed against constitutively expressed Nanoluc, to exclude trivial activators of luminescent proteins, leaving 134 hits. Cytotoxicity assays excluded immediately toxic compounds, leaving 130. While primary screening was performed in ATF4-Nanoluc lines for maximal sensitivity, hits were subsequently re-tested in a second CHO ATF4::luc2 reporter line as a more stringent orthogonal assay to prioritise robust ISR activators. Of the 130 hits identified in the sensitive Nanoluc screen and passing early toxicity assessment, 89 were confirmed in the luc2 assay, consistent with enrichment for higher-amplitude ISR activators under more stringent detection conditions. In subsequent mechanistic studies, the ATF4-Nanoluc reporter was again used to take advantage of its higher sensitivity and simpler assay format for multi-condition comparisons.

GCN2-deficient ATF4::NanoLuc CHO reporter cells were generated by introducing the reporter into *Eif2ak4-/-* CHO cells (24). Thirty compounds were selected based on GCN2 dependency, where stimulation was lost in GCN2 null cells. Liquid chromatography-mass spectrometry (LC-MS) verified compound purity and quality leaving 16 lead compounds of high confidence from the original library stocks.

Orthogonal secondary screen

Although hits were prioritised for GCN2 dependence, we performed an additional orthogonal screen to exclude compounds that activate the ISR indirectly via ER stress, which converges on the same downstream outputs. The ISR can be activated in isolation or in combination with other stress signalling pathways, for example as part of the unfolded protein response (UPR) to ER stress (2). To distinguish between inducers of ER stress and selective activators of the ISR, we used dual reporter CHO cells that express a fluorescent ISR reporter (CHOP::GFP) and a reporter of IRE1 activity (XBP1::Turquoise) (39). Histidinol served as a positive control for ISR activation via GCN2, while tunicamycin was used to induce ER stress and activate the UPR. *Eif2ak4*$^{-/-}$ CHO cells were used to assess GCN2 dependence, while *Ppp1r15a*$^{-/-}$ cells, which are impaired in the dephosphorylation of eIF2α, were used to amplify the effects of ISR activation. Histidinol selectively activated the CHOP::GFP ISR reporter in wildtype and *Ppp1r15a*$^{-/-}$cells, but not in GCN2 deleted cells, validating this system (Figure 2A). Activation of the ISR by tunicamycin was exaggerated in the *Ppp1r15a*$^{-/-}$ cells owing to their defective dephosphorylation of eIF2α (wild type vs *Ppp1r15a-/-*, $p<0.05$). Tunicamycin activated both the CHOP::GFP and XBP1::Turquoise reporter in all three genotypes.

The 16 lead compounds were next examined both in the presence and absence of a submaximal concentration of histidinol. Using this orthogonal approach, three compounds were found to be GCN2 selective activators of the ISR (Figure 2B&C). Those which induced ER stress or showed minimal GCN2 dependence are not shown. Reporter activation was measured by fluorescence activated cell sorting (FACS) after 18 hours of treatment with 30μM compound 18, 20μM compound 20, and 7.5μM compound 21. The three GCN2 selective activators included compound 18, *N-(4-*

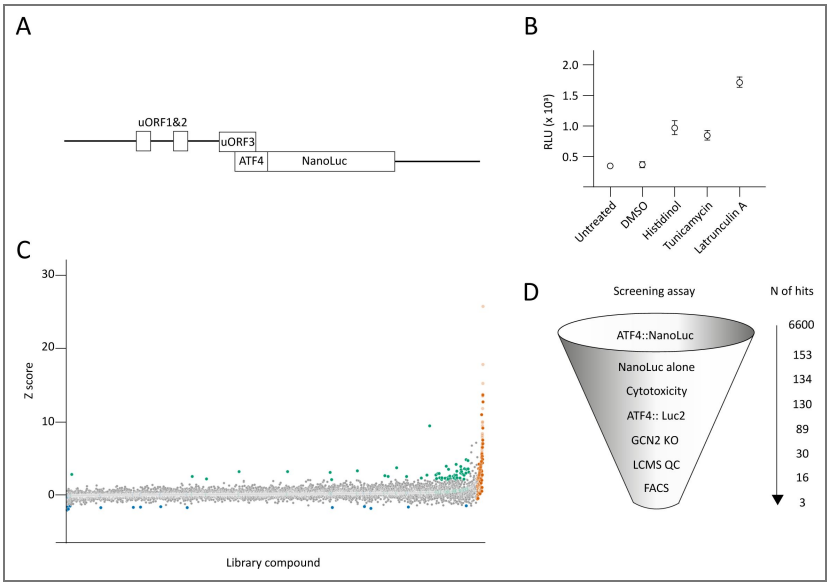

Figure 1. Chemical Screen of novel GCN2-specific ISR-activating molecules.

(A) Schematic of ATF4::NanoLuc reporter, exploiting the upstream open reading frames (uORFs). Short uORFs 1, 2 and 3 precede the ATF4 translation start site, with uORF3 overlapping the ATF4 coding sequence, but out-of-frame. During the ISR, skipping of uORF3 leads to increased translation initiation at the ATF4 initiator AUG. (B) Relative Light Unit (RLU) of ATF4 signal in CHO stable cell-line overexpressing ATF4::NanoLuc treated with 1mM histidinol, 2.5 µg/mL tunicamycin, or 1 µM latrunculin A (n=3; ± SEM). (C) Chemical screen of 6,461 small molecules tested with CHO stable cell-line overexpressing ATF4::NanoLuc. The molecules were treated alone or with submaximal ISR activation with 0.3mM histidinol. All molecules were displayed along the x-axis based on their Z-score of relative reporter signal when treated with compound alone (pale symbols). Z-score for treatment with compound and histidinol is also plotted at the same x-axis position (dark symbols). Molecules with Z-score > 3 (i.e., over 3 standard deviations from the mean reporter signal) were identified as hits: ISR activator in orange and ISR augmenter (exaggerating ISR activation by histidinol) in green. (D) Pipeline of molecule short-listing, primary screening using CHO ATF4::NanoLuc reporter (153 hits), NanoLuc alone control (134 hits), selection based on cytotoxicity (130 hits), orthogonal CHO ATF4::FLuc reporter (89 hits), and subsequent GCN2 specificity in GCN2 null reporter cells (30 hits) and compound quality control via LC-MS (16 hits), finally validation by GCN2-specific FACS to a short list of 3 compounds.

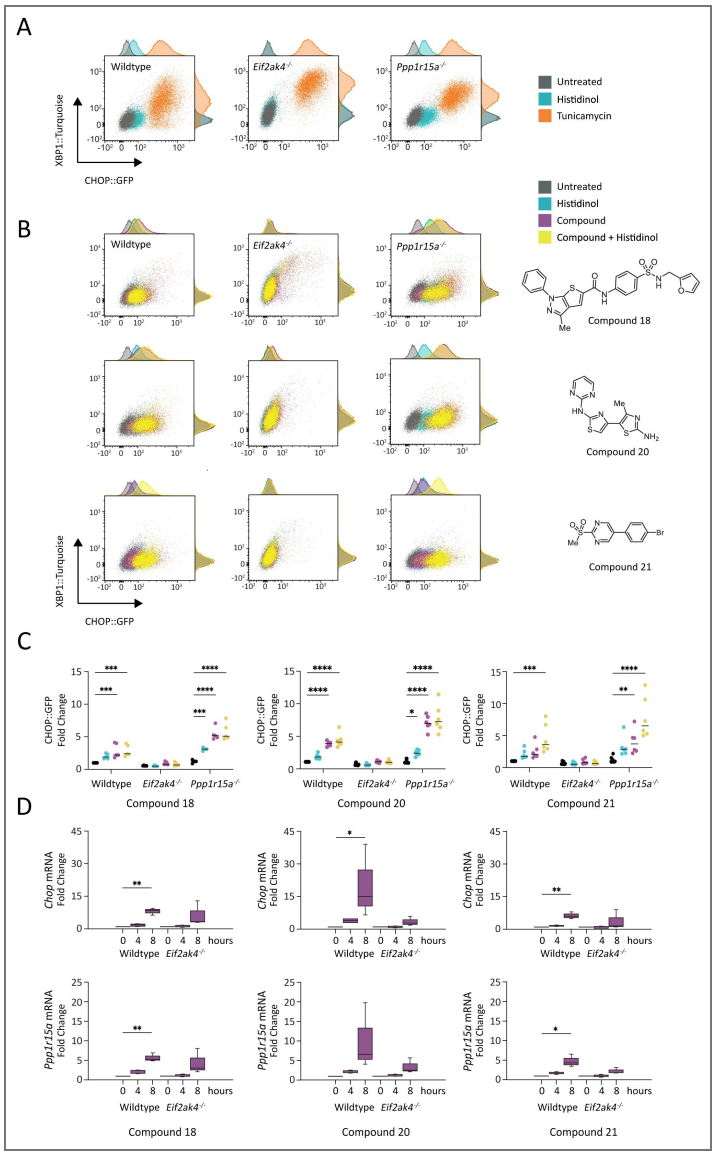

Figure 2. Shortlist and characterisation of three top hits (compound 18, 20, and 21)

(A) Representative dot plot of flow cytometry data in CHO CHOP::GFP and XBP1::Turquoise dual-reporter wildtype, *Eif2ak4*Δ, and *Ppp1r15a*Δ cells under 18-hour treatment of 0.75mM histidinol (blue), 2μg/mL tunicamycin (orange), and untreated control (gray) (n=2). Bi-exponential display was used for the plots. The x-axis represents fluorescence signals at 530nm for GFP (CHOP reporter) and y-axis represents fluorescence signals at 450nm for turquoise (XBP1/IRE1 reporter). (B) Representative bi-exponential displayed dot plot of flow cytometry data in CHO CHOP::GFP and XBP1::Turquoise dual-reporter wildtype, *Eif2ak4*Δ, and *Ppp1r15a*Δ cells under 18-hour treatment of 30μM compound 18, 20μM compound 20, and 7.5μM compound 21 alone (magenta) or in combination with 0.75mM histidinol (yellow) (n=6). Histidinol alone is shown in blue and untreated in grey. The x-axis represents fluorescence signals at 530nm for GFP (CHOP reporter) and y-axis represents fluorescence signals at 450nm for turquoise (XBP1/IRE1 reporter). Structures of compounds 18, 20, and 21 shown on the right. (C) Quantification of B (n=6); Two-way ANOVA with Tukey's multiple comparisons test was performed and the CHOP-GFP signals (530nm) in different treatment groups were compared. *: $p \leq 0.05$, **: $p \leq 0.01$, ***: $p \leq 0.001$, ****: $p \leq 0.0001$. (D) Box and whisker plot displaying mRNA fold change of ISR effector CHOP and PPP1R15A after 4- and 8-hour treatment of 30μM compound 18, 10μM compound 20, and 10μM compound 21 as detected by qPCR (n=3). ± SEM, Two-way ANOVA was performed, * $p \leq 0.05$, ** $p \leq 0.01$.

{[(furan-2-yl)methyl]sulfamoyl}phenyl)-3-methyl-1-phenyl-1H-thieno[2,3-c]pyrazole-5-carboxamide, containing a furan and two phenyl rings; compound 20, *4'-methyl-N~2~-2-pyrimidinyl-4,5'-bi-1,3-thiazole-2,2'-diamine*, containing two aminothiazoles; and compound 21, *5-(4-bromophenyl)-2-(methylsulfonyl)pyrimidine* (Figure 2B).

Larger quantities of compound 18 were then purchased from TimTec, USA (compound ST51216373); compound 20 was synthesised by ChemBridge, USA (compound 5935953); and compound 21 was purchased from Specs, Netherlands (compound AC-907/25005415). After validating their effects using the assays described above, we next confirmed activation of the ISR by these compounds at the transcriptional level at 4 and 8 hours. CHO cells were treated with 30μM of compound 18 or 10μM of compound 20 or 21 for 4 and 8 hours and expression of the ISR target genes *Chop* and *Ppp1r15a* was measured using qPCR (Figure 2D). All three induced ISR gene expression, with compound 20 eliciting the strongest response.

Studies with compound 18 were limited by poor aqueous solubility; therefore, time-course analyses focused on compounds 20 and 21. To assess ISR activation over an extended period, live-cell luciferase measurements were performed using CHO cells stably expressing an ATF4::Nanoluc-PEST reporter. Both compounds elicited maximal reporter activation between 6 and 8LJhours (Figure S1A&B). Compound 20, but not 21, induced a significant GCN2-dependent reduction in mRNA translation, as measured by puromycin incorporation, with a progressive effect observed up to 7LJhours (Figure S1C-F).

Cell line differences in GCN2 activator potencies

Neratinib is an ATP-competitive pan-HER kinase inhibitor used clinically in the treatment of breast cancer (40). Recent studies have shown that the sensitivity of glioblastoma cells to neratinib is dependent on GCN2, with GCN2 activation observed at submicromolar concentrations but inhibition at higher concentrations (26). We reproduced this biphasic activation of the ISR reporter in human cervical carcinoma HeLa cells and hamster CHO cells, recording EC_{50} values for activation of 269nM (95% CI 218-322nM) and 690nM (95% CI 634-772nM) respectively (Figure 3A). Disruption of the *EIF2AK4* gene by CRISPR/Cas9 (*EIF2AK4*$^{-/-}$) in HeLa cells abrogated ISR activation confirming the effect to be mediated by GCN2 (Figure 3A, middle panel).

In CHO cells, compound 18 was the least potent with an EC_{50} of greater than 30μM without obvious inhibition up to 100μM (Figure 3B). Notably, compound 18 failed to activate the ISR measurably in either HeLa cells or human embryonic kidney 293T cells (Figure 3C). Compound 20 activated the ISR in CHO cells in a biphasic manner with an EC_{50} of 4.8μM (95% CI 4.0-5.6μM) (Figure 3B). It was active in 293T cells though with a lower potency, EC_{50} of 17μM, but was inactive in HeLa cells (Figure 3C). Compound 21 also showed biphasic activation of the ISR in CHO cells with an EC_{50} of 5.0μM (95% CI 3.9-6.5μM) (Figure 3B). Weak activation was observed in 293T cells, but none was seen in HeLa cells (Figure 3C). To benchmark ISR activation in these models, each cell type was treated with 3mM histidinol (Figure S2). Reporter activation was most robust in CHO cells, followed by 293T cells, then HeLa cells.

GCN2iB, a potent inhibitor of GCN2, abolished histidinol-induced activation of the ATF4::NanoLuc ISR reporter in CHO cells confirming this to be GCN2 mediated (Figure 3D). Supporting a role for GCN2 in mediating the compounds' effects, GCN2iB substantially reduced ISR reporter expression by each, though this effect was only partial at concentrations of compound 20 above 10μM (Figure 3D). This might indicate GCN2-independent effects or an ability to partially outcompete GCN2iB for binding at higher concentrations.

We went on to examine downstream cellular consequences of GCN2 activation in multiple models. While compounds did not induce detectable ISR signalling in HCT116 or COS-7 cells under the conditions tested, induction of PPP1R15A was observed in Mesobank T12 primary mesothelioma cells, indicating context-dependent biological responses. Moreover, in contrast to GCN2iB (17), the current compounds did not activate disease-associated GCN2 variants linked to PVOD [data not shown].

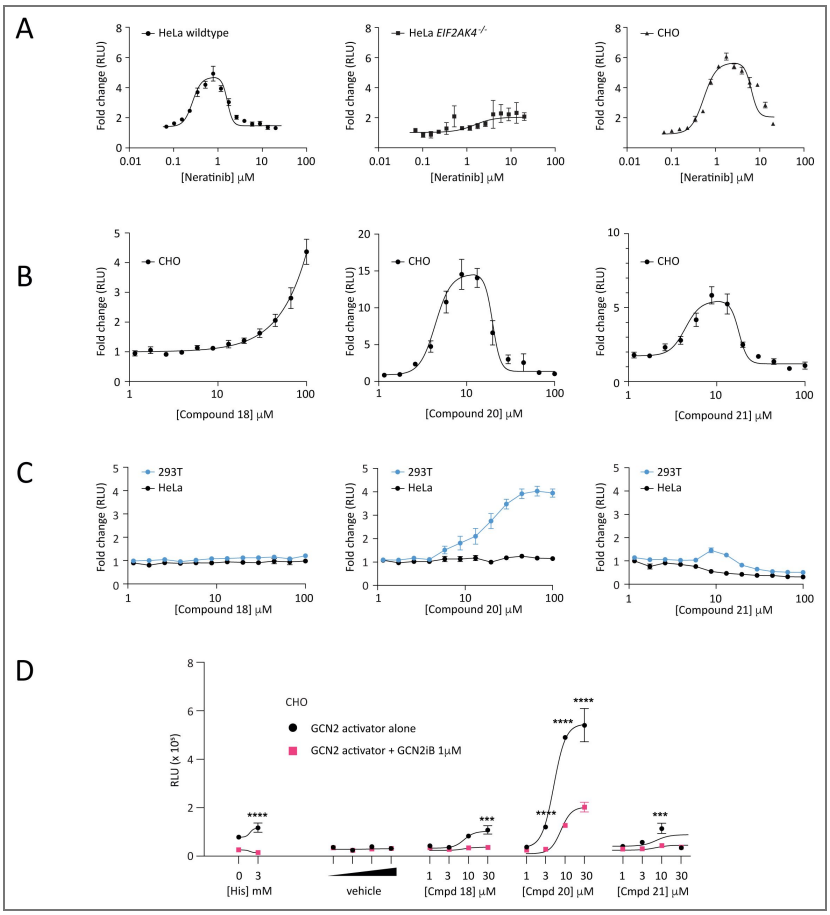

Figure 3. Compound 18, 20, and 21 display cell type-specific differences in ISR activation.

(A) Normalised dose-dependent fold change in ATF4 expression by neratinib in HeLa WT, HeLa *EIF2AK4*Δ, and CHO WT ATF4::NanoLuc reporter cells after 16-hour treatment (n=3; mean ± SEM). DMSO was used as vehicle. (B) Normalised dose-dependent fold change in ATF4 expression by compound 18, 20, and 21 in CHO WT ATF4::NanoLuc reporter cells after 16-hour treatment (n=3; mean ± SEM). EC_{50} was estimated using 4-parameter non-linear regression. DMSO treatment was used as vehicle. (C) Normalised dose-dependent fold change in ATF4 expression by compound 18, 20, and 21 in HeLa (black) and 293T (blue) WT cells transiently transfected with ATF4::NanoLuc reporter after 16-hour treatment (n=3, ± SEM). DMSO treatment was used as vehicle. (D) Relative Light Unit (RLU) of of ATF4 signal in CHO WT ATF4::NanoLuc reporter cells treated with 1, 3, 10, 30μM Compound 18, 20, and 21 alone (black) or in combination with 1μM GCN2iB (pink) for 18 hours (n=3; ± SEM). 0.01, 0.03, 0.1, 0.3% DMSO served as vehicle and 3mM histidinol as positive control. Two-way ANOVA was performed *** p≤0.001, **** p≤0.0001.

Compound 20 activates GCN2 in a GCN1-independent manner

GCN1 mediates the interaction between stalled ribosomes and GCN2 (21, 41). Histidinol is a competitive inhibitor of the histidyl-tRNA synthetase that depletes the cell of charged histidyl-tRNA, thus causing ribosome stalling and activation of the ISR in a GCN1-dependent manner (41–43). Using GCN1 deficient human 293T cells transiently expressing the ATF4::NanoLuc reporter, we confirmed that activation of the ISR by histidinol requires GCN1 (Figure 4A). Low concentrations of GCN2iB (5-70nM) had minimal effect on ISR reporter activation, while neratinib robustly triggered the ISR. The stimulatory effects of neratinib were significantly attenuated in GCN1 deficient cells consistent with the observation that GCN1 knockout renders astrocytoma cells resistant to neratinib (26). By contrast, activation of the ISR by compound 20, chosen for having the largest effect size in 293T cells, did not require GCN1 to activate the ISR reporter (Figure 4A). Indeed, loss of GCN1 modestly increased ISR activation at the highest concentration of compound 20 suggesting a mode of action independent of ribosome stalling. To gain confidence in this observation, we inactivated the *Gcn1* gene in CHO cells by CRISPR/Cas9. Neratinib-induced activation of the ATF4::NanoLuc ISR reporter was lost in GCN1 deficient CHO cells; however, ISR activation by compound 20 was completely insensitive to loss of GCN1 (Figure 4B).

No systematic assessment of GCN1 dependence has previously been performed for GCN2 activating drugs. We therefore proceeded to test a panel of ten additional kinase inhibitors that had been reported to activate GCN2 (9, 11, 26). Our panel included examples of multi-targeted tyrosine kinase inhibitors (dovitinib, sunitinib), RAF inhibitors (LY3009120, dabrafenib), inhibitors of the Wee1 kinase involved in G2 cell cycle checkpoint (WEE1-IN-4, AZD1775, Debio0123), an inhibitor of the Heat Shock Factor 1 pathway (NXP800), and EGFR inhibitors (erlotinib and gefinitinib) (9, 11, 26, 31, 44–46). In all cases, a marked reduction in GCN2 activation by the drugs was observed in GCN1 deficient cells (Figure 4C). Most of these molecules failed to activate the ISR in the absence of GCN1 (sunitinib, NXP800, dovitinib, AZD1775, dabrafenib, gefinitinib, LY3009120), while for three drugs weak activation of the ISR was seen at higher concentrations (WEE1-IN-4, Debio 0123, erlotinib). None showed the dramatic GCN1 independence observed for compound 20 in unstressed cells.

To further assess the mechanism of compound-induced ISR activation, we evaluated reporter responses in GCN2-deleted cells (Supplementary Figure S3). Several compounds, including sunitinib, NXP800, WEE1-in-4, Debio0123, gefitinib, and erlotinib, showed reduced reporter activity in GCN2-deficient cells, consistent with GCN2-dependent activation. In contrast, dovitinib, AZD1775 and dabrafenib produced weaker or inconclusive responses even in the paired wild-type lines, limiting analysis. These data allow us to distinguish compounds consistent with direct or GCN2-dependent activation from those more likely to induce ISR indirectly through cellular stress upstream of GCN2. These findings support a distinction between compounds that activate the ISR through GCN2-dependent mechanisms and those that likely act indirectly via alternative stress pathways.

ATP-competitive interaction with the GCN2 kinase domain

Existing activators of GCN2 have been shown to interact with the ATP binding pocket (9, 11, 26). We therefore used a bioluminescence resonance energy transfer (BRET)-based assay to examine the interaction of the three lead compounds with the kinase domain of GCN2 in cells. Briefly, the N-terminal portion of human GCN2 kinase domain fused to NanoLuc luciferase was expressed in either CHO or 293T cells. These were then treated with an ATP-binding pocked tracer. In this system, energy transfer is proportional to tracer binding to the NanoLuc-tagged kinase domain, and so interactions of other molecules that displace the tracer reduce the BRET ratio (Figure 5A) (47). In both CHO and 293T cells, GCN2iB efficiently suppressed the BRET ratio thus validating the system (Figure 5B). All three lead compounds significantly reduced the BRET ratio, though unlike GCN2iB, compounds 18 and 20 were noticeably more effective in CHO than in 293T cells. Although compound 21 suppressed BRET in both cell types, its effect was less dramatic in CHO

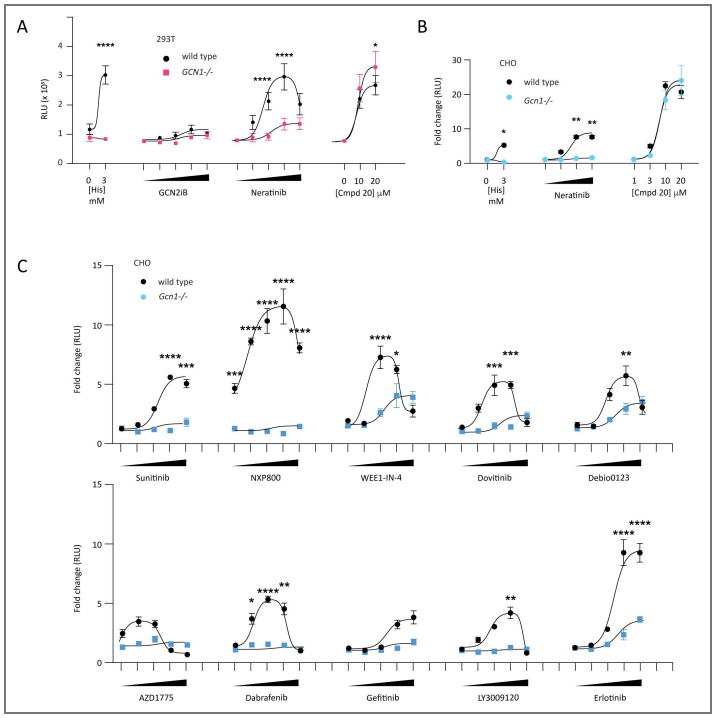

Figure 4. Compound 20 displays GCN1 independence.

(A) Relative Light Unit (RLU) of ATF4 signal in 293T WT (black) and GCN1Δ (magenta) cells transiently transfected with ATF4::NanoLuc reporter for 16-hour treatment with compound 20 (10 and 20µM), GCN2iB (5, 10, 35, 75nM), and neratinib (75, 200, 500, 1000nM) (n=3; ± SEM). Two-way ANOVA was performed * p≤0.05, ** p≤0.01, *** p≤0.001, **** p≤0.0001. (B) Normalised fold-change in ATF4 signal in CHO WT (black) and *Gcn1-/-* (blue) ATF4::NanoLuc reporter cells for 18-hour treatment with compound 20 (1, 3, 10 and 30µM) and neratinib (75, 200, 500nM) (n=3; ± SEM). Two-way ANOVA * p≤0.05, ** p≤0.01. (C) Normalised fold-change in ATF4 signal in CHO WT (black) and *Gcn1-/-* (blue) ATF4::NanoLuc reporter cells treated for 19-hours with a panel of ATP-competitive kinase inhibitors reported to activate GCN2 (0.1, 0.3, 1, 3, and 10µM) (n=3-9; mean ± SEM). Two-way ANOVA was performed * p≤0.05, ** p≤0.01, *** p≤0.001, **** p≤0.0001.

cells compared to compounds 18 and 20. The concentrations required to detect target engagement in NanoBRET assays did not directly mirror those required for ISR activation, reflecting the distinction between ligand binding and downstream pathway output.

To examine further the interaction of compounds 18 and 20 with GCN2's kinase domain, we generated in bacteria a recombinant protein comprising Glutathione S-transferases (GST) fused to the kinase domain of human GCN2 (residues 585 to 1005 of NCBI reference Sequence NP_001013725.2). GST was chosen both to facilitate protein purification, and to enhance dimerisation of the kinase domain in order to cause autophosphorylation and constitutive activation. When incubated *in vitro* with increasing concentrations of ATP and a fixed quantity of His6-tagged bacterially expressed eIF2α N-terminal domain (48), GST-GCN2 kinase domain phosphorylated its substrate on serine 51, as detected by immunoblotting (Figure 5C). Neratinib dose-dependently inhibited eIF2α phosphorylation (Figure 5D, lanes 1-5). The lack of activation by neratinib likely reflected the requirement for autoinhibitory domains of GCN2 to observe this effect. Therefore, in this system inhibition of eIF2α kinase activity was used as a surrogate for target engagement. Compounds 18 and 20 also inhibited eIF2α phosphorylation, while compound 21 appeared inactive in this assay (Figure 5D). Compounds 18 and 20 altered the apparent kinetic parameters of GCN2, including an increase in the observed V_{max}; however, these data do not allow assignment of a specific inhibition modality (Figure 5E&F).

To test the ability of compound 20 to activate full-length GCN2, we next generated full-length human GCN2 (uniprot ID: Q9P2K8) through baculoviral expression using an N-terminal twin StrepII tag. Despite exerting only a modest effect on GCN2 autophosphorylation at T899 within the activation loop, compound 20 robustly triggered the phosphorylation of full-length eIF2α to an even greater extent than purified tRNAs, a known endogenous stimulus of GCN2 activity (Figure 5G). Of note, uncharged tRNA produced a modest (~4-fold) activation of GCN2 under these conditions, whereas compound 20 induced substantially greater (~40-fold) activation.

Interaction with other ISR kinases

The eIF2α kinases have a common evolutionary origin and consequently the kinase domains share some structural similarity (49). We therefore examined the effect of the compounds on all four eIF2α kinases *in vitro*. Lower concentrations of ATP (10μM for GCN2, 0.1μM for PERK, 0.15μM for HRI, 0.1μM for PKR) were used to accentuate antagonism at the ATP site. This assay was performed at low ATP concentrations to sensitise detection of ATP-competitive inhibition and was not optimised to detect compound-mediated activation of GCN2. Under these conditions, in contrast to Figure 5G where 100μM ATP was used, activation of GCN2 is not observed with any of the compounds tested. At low ATP, full length, purified GCN2 was efficiently inhibited by GCN2iB with an IC_{50} on 1.55nM. None of the screen hits reached 50% inhibition at the highest concentration tested (3μM) though compound 20 and to a lesser extend 18, appear to cause weak inhibition (Figure 6A). No inhibition was observed with the test compounds again purified PERK (Figure 6B). The PERK inhibitor GSK2606414 served as a positive control with an expected IC_{50} of 0.66nM. Weak inhibition of HRI by compounds 18 and 20 was observed but failed to reach 50% (Figure 6C). In this system, GCN2iB was found to inhibit purified HRI with an IC_{50} of 2.76nM, similar to that observed against GCN2. By contrast, both compounds 18 and 20 inhibited PKR *in vitro*: compound 18 with an IC_{50} of 4.50μM and compound 20 with an IC_{50} of 3.75μM (Figure 6B-D). GCN2iB inhibited PKR with an IC_{50} of 3.26μM. Compound 21 was inactive against each of the four eIF2α kinases in this assay.

In silico docking of compounds 18 and 20 to the GCN2 kinase domain and structure-activity relationship (SAR) analysis

We used the SiteMap module from Schrodinger Suite to identify binding sites based on drug interactions with nearby GCN2 residues. Published crystals structures of the GCN2 kinase domain (see methods) show the ATP binding pocket comprises a large solvent exposed region and a buried hydrophobic region that extends beyond the gatekeeper residue (Met802) and towards the αC-helix (Figure 7). Compound 18 was predicted to occupy a similar pocket to that of the ligand in

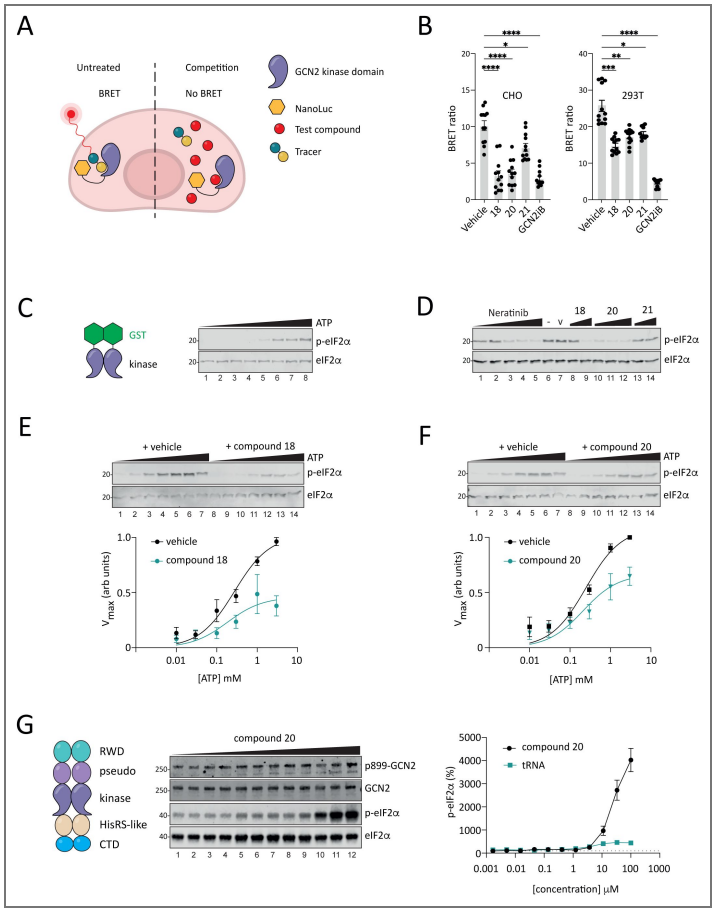

Figure 5. Compound 18 and 20 directly bind to GCN2 in cellulo and in vitro

(A) Illustration of the NanoBRET assay. Left panel displays BRET signal at baseline with tracer binding to GCN2; right panel displays reduced BRET signal due to the addition of a competitive compound that outcompetes the tracer from binding to GCN2. (B) BRET ratio in CHO and 293T WT cells with 2-hour treatment of 3% DMSO, 100μM compound 18, 20, and 21 or 0.5μM GCN2iB. (n=3; ± SEM). Two-way ANOVA was performed. *: p ≤ 0.05, **: p ≤ 0.01, ***: p ≤ 0.001, ****: p ≤ 0.0001. (C) Schematic of GST-GCN2 fusion protein (residues 585–1005) and representative immunoblot of *in vitro* kinase assay. Purified GST-GCN2 was incubated with eIF2α-NTD (residues 2–187) using a ramp of ATP concentrations (0, 0.01, 0.03, 0.1, 0.3, 1, 3, 10mM) (n=3). Total and serine51 phosphorylated eIF2α were detected. (D) Representative immunoblot of *in vitro* kinase assay showing inhibition of eIF2α-NTD (residues 2–187) phosphorylation. Purified GST-GCN2 and eIF2α-NTD was incubated with neratinib (0.075, 0.68, 6.67, 10, 20μM) and compound 18 (100-500μM), compound 20 (100, 200, 500μM), and compound 21 (100-500μM) (n=3). 5% DMSO used as vehicle control. Total and serine51 phosphorylated eIF2α were detected. Molecular size in kDa. (E) Representative immunoblot of *in vitro* kinase assay (n=3) showing inhibition of eIF2α-NTD (residues 2–187) phosphorylation by 300μM compound 18 using a ramp of ATP concentrations (0.01, 0.03, 0.1, 0.3, 1, 3, 10mM); 3% DMSO used as vehicle control. Bottom panel showed Michaelis-Menten kinetics analysis of DMSO control (black) vs compound 18 (green). Molecular size in kDa. (F) Representative immunoblot of *in vitro* kinase assay (n=3) showing inhibition of eIF2α-NTD (residues 2–187) phosphorylation by 100μM compound 20 using a ramp of ATP concentrations (0.01, 0.03, 0.1, 0.3, 1, 3, 10mM); 3% DMSO used as vehicle control. Bottom panel showed Michaelis-Menten kinetics analysis of DMSO control (black) vs compound 20 (green). Molecular size in kDa. (G) Schematic of full-length GCN2 protein and representative immunoblot of *in vitro* kinase assay. Purified full-length GCN2 was incubated with full-length eIF2a using a ramp of compound 20 or tRNA concentrations (0, 0.001, 0.005, 0.01, 0.05, 0.13, 0.4, 1.2, 3.7, 11, 33, 100μM) (n=3). Total and serine51 phosphorylated eIF2a, as well as total and threonine899 phosphorylated GCN2 were detected. On the right showed quantification of serine51 phosphorylated eIF2a with a ramp of tRNA (black) vs compound 20 (green). Molecular size in kDa.

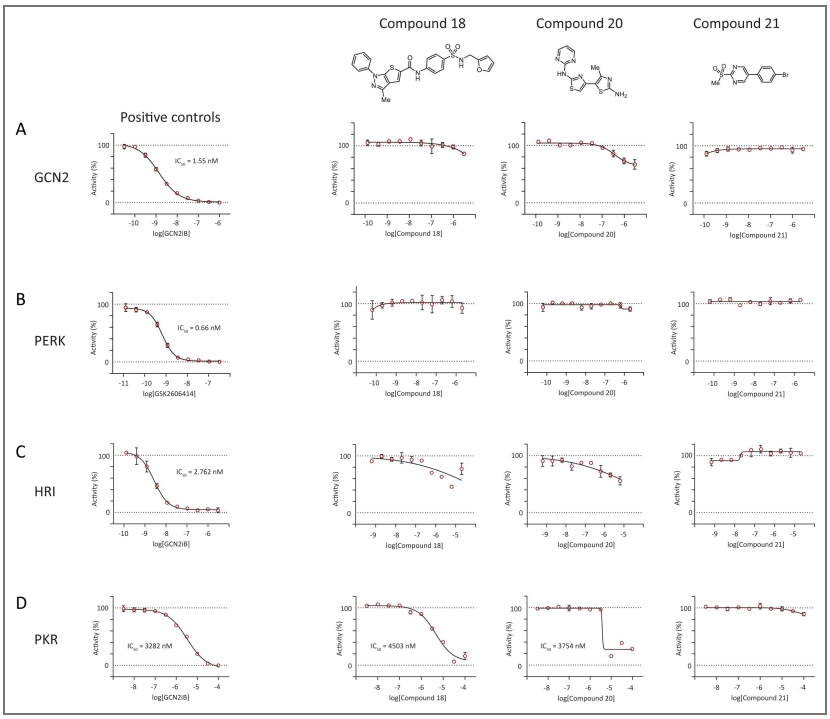

Figure 6. **Compound activity across eIF2α kinases using *LanthaScreen in vitro kinase activity assay***

Left panels: dose-dependent inhibition of GCN2, PERK, HRI or PKR with positive control drug GCN2iB or GSK2606414. Right panels: effect of concentration ranges of compounds 18, 20, and 21 in this system revealed weak inhibition of GCN2, HRI, and PKR. Low ATP concentrations were used to accentuate inhibition, and this masks the stimulatory effects on GCN2.

the PDB 6N3N crystal structure demonstrating a Type 1.5 binding configuration, characterised by the DFG loop being “in” and the αC-helix being in the “out” conformation (10). The furan motif of compound 18 was predicted to be buried in the allosteric pocket around αC-helix, between gatekeeper Met802 and Leu640 (Figure 7D). The compound’s sulfone was predicted to interact with Phe867 of the conserved DFG-motif. In neratinib, a triad of hydrogen bonding was predicted between the 8-position of the isoquinoline core (Ar-H bond), the amine linker (H bond) and the 2-position of the fluorobenzene ring (Ar-H Bond) with Asp866, similar to the predicted interaction between the amide linkage of compound 18 and Asp866 (Figure 7B). Both neratinib and compound 18 were also predicted to protrude into the solvent exposed space (Figure 7B-E). However, the interaction of neratinib with Cys805 of the hinge region through the nitrile of isoquinoline core was not present in compound 18.

Due to the metabolic liabilities of furans in medicinal chemistry programs, we sought to explore the importance of this motif for binding and activity using available structural analogues. Replacement of the sulfonamide furan motif with some benzene derivatives including phenolic (BCC0106222), 2-bromobenzene (BCC0113320), 3-acetylbezene (BCC0104214), preserved ISR activation while others (BCC0073242 and BCC0043997) resulted in a loss of activity (Supplementary Table 1). Incorporation of heterocyclic ring systems (BCC0073142, Z56783036) or modification of solvent exposed region (Z88478561, Z226209130, Z11741677) were similarly not tolerated (Supplementary Table 1). However, modifying the furan motif to benzene derivative 2-bromobenzene (BCC0113320) and heterocyclic ring (BCC0077119) preserved GCN2-specific ISR activation.

Unlike compound 18 and neratinib, compound 20 was not predicted to protrude into the allosteric pocket (Figure 7F&G). Analogues extending further towards the αC-helix and protruding into the solvent-exposed region were inactive (e.g., Z118606822), suggesting that the small size of compound 20 may be advantageous, fitting into the ATP-binding pocket of GCN2 and facilitating stronger activation (Supplementary Table 1). Hydrogen bond interaction was predicted between the NH_2 of the compound 20 aminothiazole with the carbonyl of the hinge region Cys805. Additional interaction was predicted between the linker NH of compound 20 and backbone carbonyl of Asp866 in the DFG-motif. Such 2-aminopyrimidine rings are present in many kinase ligands (50). Rather than this interacting with hinge region residues, this moiety in compound 20 was predicted to form a pi-cation interaction with Lys619 and a hydrogen bond with DFG Asp866, as has been reported for other ligands of kinase ATP pockets (10). Replacement of this pyrimidine ring with 2-pyridine analogues (BCC0084738, BCC0079350 and BCC0083923) was well tolerated, likely due to the conserved hydrogen bonding interaction between the pyridine nitrogen and Asp866. Removal of a nitrogen from the ring system, such as BCC0057014, BCC0089519, BCC0084744, and BCC0084833 all resulted in a loss of activity, possibly due to their lack of interaction with Asp866 (Supplementary Table 1). Due to toxicity issues surrounding 3-aminothiazoles, modifications were made to replace the terminal thiazole ring system with phenyl derivatives (BCC0080152, BCC0075509, BCC0084830, BCC0057431 and BCC0080200). However, these resulted in a decrease in activity towards GCN2, suggesting that there might be a steric component contributing to activity. Replacing the thiazole with a minimally steric affecting thiophene (BCC0079876) also led to activity loss, possibly due to the twisting of central thiazole ring that impaired hydrogen bonding between pyrimidine nitrogen and Asp866. We were therefore unable to improve upon compound 20’s activity but gained valuable SAR information for future development.

To provide additional context on the developability of the identified compounds, we performed an *in silico* assessment of key physicochemical and pharmacokinetic properties. Predicted blood–brain barrier (BBB) permeability scores suggested a gradient across compounds, with compound 18 scoring 5.13 (indicative of a high likelihood of central nervous system penetration), compound 20 scoring 4.29 (moderate predicted penetration), and compound 21 scoring 3.35 (lower likelihood of brain exposure), consistent with its greater polarity. Analysis of lipophilicity, reflecting how readily a compound partitions into lipid membranes, showed that compound 18 has relatively balanced properties (cLogP 1.84; logD 1.98) but very low aqueous solubility (0.07), which may limit

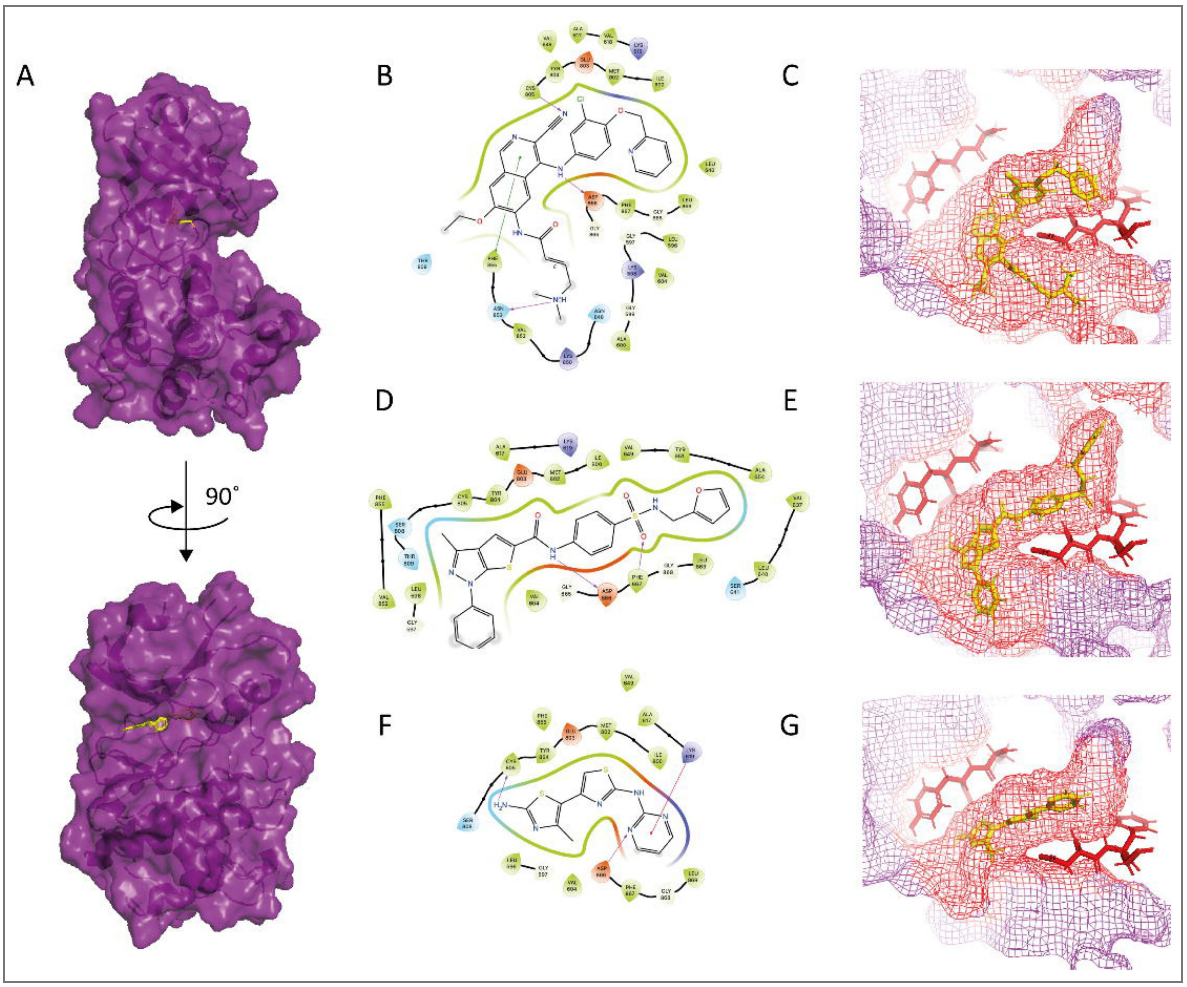

Figure 7. **Structural modelling**

(A) Illustration of GCN2 kinase domain from up (N-terminus) to down (C-terminus) with illustrative ligand (yellow) in ATP-binding pocket. (B) 2D ligand interaction diagram of neratinib, (D) compound 18, and (F) compound 20. Violet, green, and red colored lining indicate hydrogen bond, π-π, and cation-π interactions, respectively. Polar and hydrophobic residues are highlighted in blue and green, respectively. Mesh representation of the ATP-binding pocket in GCN2 kinase domain was shown with ligand (yellow): (C) neratinib, (E) compound 18, and (G) compound 20. Key residues surrounding the ATP-binding pocket, including the DFG motif (D866-G868) and EYC residues (E803-C805) following the gatekeeper M802 were labelled red. Figures adapted from crystal structure 6N3N.

bioavailability. Compound 20 exhibited more moderate lipophilicity alongside improved solubility (0.67), whereas compound 21 was the most lipophilic and the least soluble, indicating a less favourable balance of properties. As expected, solubility decreased with increasing molecular weight and lipophilicity. Taken together, these data indicate that compound 20 achieves the most favourable balance between solubility, lipophilicity, and predicted tissue distribution, consistent with a more drug-like profile and supporting its prioritisation for further development.

Discussion

The ISR plays a critical role for maintaining homeostasis under diverse stress conditions and its disruption results in a variety of disease states (2). The observation that some pathogenic variants of GCN2 are amenable to pharmacological activation led us to seek novel GCN2 activators. Our chemical screen identified three chemically distinct GCN2 activating molecules, one of which is, to our knowledge, the first to show independence from GCN1 for its activity. This may prove useful as a tool compound for the study of GCN2 in cells and using purified components since it overcomes at least one hurdle to kinase activation.

Recent work suggests that the ATP-competitive modulator GCN2iB can activate GCN2 independently of GCN1 under specific conditions using a GCN2 E26A mutant (9). In our hands, we did not observe GCN1-independent activation with GCN2iB at the concentrations tested. This discrepancy may reflect a narrow concentration window for GCN1-independent activation or context-dependent effects of the E26A mutation. These findings raise the possibility that GCN1-independent activation of GCN2 may occur under specific conditions or with distinct classes of compounds.

Compounds 18 and 20 demonstrate weak inhibition of the related kinase PKR. Previous structural analyses have shown the kinase domains of PKR and GCN2 to be highly conserved, particularly at the ATP-binding pocket, which likely contributes to this effect. Indeed, a previous publication reported that other small molecule inhibitors of GCN2, including a series based on a triazolo[4,5-d]pyrimidine scaffold, demonstrated cross-inhibition of PKR (51). Furthermore, the PKR inhibitor C16 has been shown to activate GCN2 *in vitro* (11). Intriguingly, viral infections or synthetic dsRNA known to activate PKR, have also been shown to trigger GCN2 in some circumstances, though if this relates to structural similarities of their kinase domains has not been studied (11, 52, 53). While the functional relevance of PKR inhibition in our cellular systems is uncertain, these observations highlight the potential for kinase cross-reactivity, which will be important to address in future studies.

A remarkable finding in the current study was the lack of dependence on GCN1 for compound 20 to activate GCN2 in cells. During amino acid starvation, ribosome-associated GCN1 facilitates binding of uncharged tRNAs to GCN2, thus facilitating GCN2 activation (21, 54, 55). GCN1 also functions as a disome detector, enabling GCN2 activation in response to ribosome collisions (41). In genetic screens identifying modifiers of GCN2 activation by a small molecule, such as the dual HER2/EGFR inhibitor neratinib and the WEE1 inhibitor AZD1775, GCN1 has repeatedly been found to be necessary (26, 30, 31). We were able to confirm this GCN1 dependence for neratinib in the present study. It was therefore surprising that GCN2 activation by compound 20 did not appear to require GCN1 in human or hamster cells. While GCN1 is essential for the activation of GCN2 by amino acid starvation in yeast (56, 57), *in vitro* studies have shown that GCN2 activation by the ribosome P-stalk or by deacylated tRNAs does not absolutely require GCN1 (24, 25). Yet we found compound 20 able to activate purified full-length human GCN2 to a far higher level than was possible with purified tRNAs. The markedly greater activation observed with compound 20 compared with uncharged tRNA *in vitro* raises the possibility that such compounds may partially bypass regulatory constraints on GCN2 activation, including those normally mediated by GCN1. Our modelling suggests that unlike neratinib, compound 20 can fit within the ATP-pocket without needing to protrude into the solvent, nor extending deeply into the hydrophobic region beyond the gatekeeper Met802 residue towards the αC-helix. Indeed, analogues extending in these directions were inactive, perhaps suggesting value to this molecule's small size. This may prove useful as a tool compound for studies in which GCN1 is unavailable or non-functional.

There are limitations to our study. So far, our experiments have been limited to cultured cells, purified proteins, and *in silico* modelling. We have yet to test our compounds in an animal model. Although our pipeline excluded molecules showing toxicity, it is likely that prolonged activation of the ISR will have toxic consequences via targets including CHOP and PPP1R15A (16). Our most promising molecule, compound 20, contains a 2-aminothiazole. Although known to be a versatile scaffold, appearing in several clinically useful drugs including anti-inflammatory, anti-microbial and anticancer agents, 2-aminothiazole is sometimes considered a toxicophore owing to toxic consequences following its metabolism, and as a pan-assay interference compound (PAINS), owing to frequent false positives in high-throughput drug screens (58–60). Our use of orthogonal approaches to support its activity as a GCN2 activator, mitigate against it being a non-specific hit. Nevertheless, if this compound were to be developed further, attempts to 'design out' this feature by, for example, replacing the sulphur for an oxygen (thiazole to oxazole switch) could be attempted. Indeed, computational modelling reveals an adjacent NH which should form a stronger H-bond to oxygen of an oxazole, which may result in an improved potency to GCN2. Another potential limitation of our study is the use of existing analogues in SAR studies, the so-called 'analogue by catalogue' approach. Although less systematic than chemically synthesising further series *de novo*, it was cost effective and generated useful information on the tolerability of modifications of our lead scaffolds. Finally, our compounds were identified in a screen of CHO cells and appear to be more effective in these cells that in HeLa and 293T models. The absence of detectable activity in HeLa cells does not appear to be a species effect, since some activity was observed in human 293T cells and when using recombinant human GCN2 protein. It is likely therefore to reflect cell-type effects, since cancer cell lines are known to demonstrate dramatic differences in drug efficiency, even when using different strains of the same cell line (61). Moreover, histidinol-induced ISR activation showed a clear hierarchy across cell lines, with CHO cells being the most responsive and HeLa cells the least. We also evaluated the reported GCN2 activator HC-7366 in our CHO ATF4::NanoLuc reporter system. In this context, HC-7366 showed limited activity relative to compound 20, despite its reported efficacy in other cellular systems and *in vivo* (data not shown). This highlights potential context dependence in small-molecule activation of GCN2 and limits direct cross-study comparison. This should be considered carefully when using these compounds as tools or for further drug development.

In summary, we performed a chemical screen for novel activators of GCN2. We identified three chemically distinct scaffolds, and demonstrated one to be independent of the GCN2 cofactor GCN1.

Methods

Screen molecules

The initial screen used compounds sourced from the BioAscent library and all molecules dissolved in DMSO. Some follow-on compounds for SAR were sourced from Enamine. Subsequently, compound 18 was purchased from TimTec, USA (compound ST51216373). Compound 20 was synthesised by ChemBridge, USA (compound 5935953). Compound 21 was ordered from Specs, Netherlands (compound AC-907/25005415).

NanoGlo® luciferase assay

pGL4.2 ATF4-Nluc and pGL4.2 ATF4-Nluc-PEST® were described previously (17). In 384-well white microplate, test compounds, 3mM histidinol or vehicle control were plated as 5x solution in a volume of 5µL in 10% FBS-Nutrient Mixture F-12 Ham supplemented with 1x GlutaMAX™. CHO wildtype and *Eif2ak4-/-* ATF4::NanoLuc reporter cells were subsequently seeded at a density of 1.5×10^3 cells per well in 20µL. After 16 hours at 37°C, NanoGlo® luciferase assay reagent was added to each well and mixed with orbital shaking for 1 minute. After 10 minutes of incubation at room temperature, bioluminescence signal (360-545 nm) was acquired on a Tecan Spark plate reader. Cells carrying a ATF4::nanoLuc-PEST reporter were used for live-cell assay, allowing detection of time-sensitive ATF4 signals (17). Cells (1.25×10^4 cells per well) were plated overnight on white, clear bottom 96-well plate. Next day, 1µL 100x Nano-Glo® Endurazine™ substrate was mixed with cell culture medium and added to cells and incubated for 2 hours to reach

stabilisation. Compounds were added to the wells and luminescence signals were measured using a Tecan CM Spark plate reader at 37°C in a humidity cassette for 48 hours. Data analysed using Graphpad Prism 10.

Bioluminescence Resonance Energy Transfer (BRET)

NanoBRET assay was performed according to user's manual. Briefly, 4×10^5 cells/mL (HEK293T or CHO) were transfected with 100ng of GCN2 kinase domain::nanoLuc reporter and 900ng of transfection carrier DNA mixed in 100µL Opti-mem (no phenol red) using lipofectamine LTX, and plated in 384-well cell-culture white microplates (40µL/well, 8×10^3 cells). Twenty-two hours after transfection, tracer was added to each well and mixed on an orbital shaker. Test compound (final concentration 10, 30, 100µM), DMSO control (final concentration 0.1, 0.3, 1%), and positive control GCN2iB (final concentration 1µM) were added to each well and mixed. After 2 hours of incubation, NanoBRET™ Nano-Glo® substrate-extracellular NanoLuc® Inhibitor reagent was added to each well before bioluminescence measurement using a Tecan CM Spark plate reader (multi-colour measurement mode: wavelength 1, wavelength 445-470nm, 300ms integration; wavelength 2, wavelength 610-635nm, 300ms integration). Data analysed using Graphpad Prism 10.

Cell Viability Assay

Compounds were plated into 384-well white microplates and mixed with 20µL of culture medium containing 1.5×10^3 cells per well, incubated for 16 hours at 37°C. CellTiter-Glo® Assay reagent was added to each well for bioluminescence measurement using a Tecan CM Spark plate reader. Data analysed using Graphpad Prism 10.

Flow cytometry

CHOP::GFP and XBP1::Turquoise dual-reporter cells were treated with each compound (7.5-20µM) and histidinol (0.75mM) 18-20 hours prior to cell harvesting (39). ER stress was induced using 2µg/mL of tunicamycin. At the time of experiment, cells were trypsinised and collected by centrifugation, resuspended in 4mM EDTA PBS, filtered through a 50µm filter, then analysed using a DB Fortessa flow cytometer. GFP was measured at 530nm and Turquoise was measured at 450nm. Data analysed using FlowJo software.

Quantitative real time PCR (qPCR)

RNA was reverse transcribed to produce complementary DNA using High-Capacity cDNA Reverse Transcription Kit (Thermo, 4368814) according to the manufacturer's instructions. To perform real-time PCR, the PowerUp SYBR Green Master Mix (Thermo A25742) and the CFX96 BioRad real-time PCR machine (Biorad, UK) were used. All samples were measured in duplicate and included water control. Fold changes in expression were calculated using the ΔΔCt method. Hamster qPCR primers include

CHOP (Fw: GGGAGCTGGAAGCCTGGTAT, Rv: GGGACCCCCATTTTCATCTG), PPP1R15A (Fw: CCTGGTC TGCAAAGTGCTGAT, Rv: CCAGCTCAGTCACTCCCTCTTC), and β-actin (Fw: ACTCCTACGTGGGTGACGA G, Rv: AGGTGTGGTGCCAGATCTTC). Data analysed using Graphpad Prism 10.

Immunoblotting

Cells were washed with PBS on ice and lysed in low-salt buffer as previously described (17). Following SDS-PAGE (7% gel for GCN2 and 14% gel for eIF2α or alternatively, 5-12% gradient gel), proteins were transferred to nitrocellulose membranes then analysed by immunoblotting. Antibodies used: total GCN2 (Gift from Ron lab: NY168); total GCN2 (1:1000, Invitrogen JA03-83); GCN2-phosphorT899 (1:1000, Abcam, ab75836); β-actin (1:5000, Abcam, ab8226); eIF2α phos-S51 (1:1000, Abcam, ab32157); eIF2α phos-S51 (1:500, Cell Signalling Technology 9721); total eIF2α (1:1000, Invitrogen, AHO0802); total eIF2α (Gift from David Ron lab, CIMR); total eIF2α (1:1000, Santa Cruz Biotechnology sc-133132).

Recombinant GCN2 kinase domain synthesis and in vitro kinase assay

The human GCN2 kinase domain (residues 585 to 1005) was tagged on its N-terminus with GST by cloning into the vector pGV67 by Gibson assembly. Protein was synthesised in BL21(DE3) E. coli Rosetta cells and purified using glutathione agarose beads. GCN2 kinase domain (0.3µg) was incubated with 100µM ATP, 1µM eIF2α-NTD and test compounds in reaction buffer (50mM HEPES, pH 7.4, 100mM potassium acetate, 5mM magnesium acetate, 250µg/ml BSA, 10mM magnesium chloride, 5mM DTT, 5 mM β-glycerophosphate). Reactions were incubated at 32°C for 10 minutes, then immediately quenched with SDS sample buffer pre-warmed to 95°C. Samples were then analysed by immunoblotting.

Recombinant full-length GCN2 synthesis and in vitro kinase assay

Expression and purification of recombinant human GCN2 was conducted as described previously (25). Briefly, human GCN2 (uniprot ID: Q9P2K8) was cloned into a baculoviral vector with an N-terminal twin StrepII tag followed by a TEV protease site. GCN2 was then expressed in *Sf9* cells grown at 27 °C for 55 hours. Protein was purified using sequential StrepTrap HP column (GE Healthcare Life Sciences 28-9075-47), HiTrap Q HP column (Cytiva 17115401), Hi Load 16/60 Superdex 200 column (Cytiva/GE Healthcare 28989335). Ten nanomolar GCN2 was incubated at 30 °C for 20 min with 2µM eIF2α and 100µM ATP in increasing concentrations (0.00169-100µM) of deacylated tRNA or compound 20. Samples were then quenched via the addition of SDS-PAGE loading buffer and heating to 95 °C for 3 min, then analysed by SDS-PAGE and immunoblotting: total eIF2α (Santa Cruz Biotechnology sc-133132) 1:1000, phospho-eIF2S1 Ser51 (Cell Signalling Technology 9721) 1:500, total GCN2 (Invitrogen JA03-83) 1:1000, pThr899 GCN2 (Abcam AB75836) 1:1000. Images were captured and quantified in Image Studio Ver 5.2. Data analysed using Graphpad Prism 10.

Expression and purification of eIF2α

Expression and purification of recombinant human eIF2α was conducted as described previously (25). DNA encoding full-length human eIF2α (NCBI reference number: NP_004085.1) was inserted into the vector pOPTH with an N-terminal His6 tag followed by a TEV protease site. Protein was expressed in BL21 Star (DE3) cells, at 37 °C for 3 hours then purified using a HisTrap HP Column (Cytiva 17524801) as described for GCN2.

LanthaScreen in vitro kinase activity assay

In 384-well plate format, 1nM human GCN2 (Carna Bioscience, # 05-153) or 1nM human PERK (Carna Bioscience, # 05-155) or 2nM human HRI (Carna Bioscience, # 05-154) or 3nM human PKR (Carna Bioscience, # 05-156) were incubated with 50mM HEPES pH 7.0, $MgCl_2$ 10mM, $MnCl_2$ 5mM, tRNA 4µM (only for GCN2 assays), ATP (10µM for GCN2, 0.1µM for PERK, 0.15µM for HRI, 0.1µM for PKR), GFP-eIF2α 80nM. Reaction time was 20-30 minutes at room temperature, followed by detection time 50-60 minutes. TR-FRET signal between terbium-labeled antibody and GFP-labeled p-eIF2α read with excitation 340nm and emission of the donor (terbium labeled anti-p-eIF2α antibody: 495 nm) and the acceptor (GFP-labeled p-eIF2α: 520nm) on the Tecan Spark plate reader. IC_{50} values were determined in GraphPad Prism 8.0, using a 4-parameter model: log(inhibitor) vs. response – variable slope.

In silico modelling

Five reported crystal structures for human GCN2 were considered (PDB 6N3N, 6N3O, 6N3L, 7QWK, and 7QQ6 (10, 62). Of these, 6N3N and 6N3L share ~100% sequence homology. While 6N3N has unresolved amino acids residues, these are remote from the ATP binding site and should not impact the binding of the ligands. A visual inspection of 6N3O, 6N3N, and 6N3L highlighted that the activation loop in 6N3L is cut short and does not extend beyond the αC-helix, affecting the orientation of the DFG loop and its residues (Asp866, Phe867, Gly868). As such, 6N3L was not

considered for further analysis. PDB sequences 7QWK and 7QQ6 share ~75% sequence homology, with 7QWK containing unresolved residues remote from the ATP binding site. As observed with PDB 6N3L, the activation loop containing the DFG residues is cut short in both cases and does not extend beyond the αC-helix. Inspection of the binding mode of crystallised ligands of 7QQ6 and 7QWK demonstrate that these bind in a Type I binding pocket, compared to Type II binding as observed in 6N3O.

Prior to docking, the protein structure (PDB ID: 6N3N) was put through the Protein Preparation Protocol of Maestro. This protocol added hydrogens, removed co-crystallised water molecules, optimised the receptor's hydrogen bond network, enumerated bond orders, and performed a restrained minimisation to alleviate backbone clashes with the receptor backbone. The protein was prepared at pH7.4 (63). SiteMap module was used on the prepared protein, with all settings set to default (SiteMap, Schrödinger Release 2024-4, Schrödinger, LLC, New York, *http://www.schrodinger.com/*). Grid generation was performed using the Glide Docking Protocol in Masestro (Glide, Schrödinger Release 2024-4, Schrödinger, LLC, New York, *http://www.schrodinger.com/*). This was centred around Met802 and Lys619. High throughput virtual screening (HTVS) setting was used for docking.

Structure of compound 18 analogue and fragment	ID	ISR activation	GCN2 specificity
NC(=O)c1ccc(cc1)S(=O)(=O)NCc1ccco1 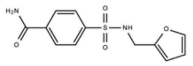	Z33546257	-	NA
CC(C)c1nnc(s1)NC(=O)c1cc2c(nn(c2s1)-c1ccccc1)C 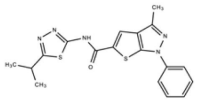	Z56783036	-	NA
CC(C)Cn1nc(c2cc(sc12)C(=O)Nc1cc(ccc1C)S(=O)(=O)C)C 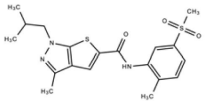	Z88478561	-	NA
Cc1nn(c2sc(cc12)C(=O)Nc1cccc(c1)CO)-c1ccccc1 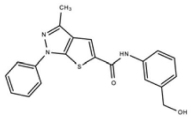	Z28913272	+	NA
Cc1nn(c2sc(cc12)C(=O)Nc1ccncc1)-c1ccccc1	Z85517350	++	NA
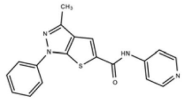			
Cc1nn(c2sc(cc12)C(=O)Nc1ccc(cc1)S(=O)(=O)N)-c1ccc(cc1)Cl 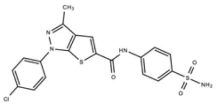	Z27682945	+	NA
COc1ccc(cn1)CNC(=O)c1cc2c(nn(c2s1)-c1ccc(cc1)F)C 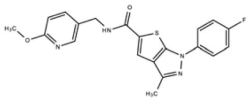	Z226209130	-	NA
Cc1nn(c2sc(cc12)C(=O)Nc1cccnc1)Cc1ccccc1 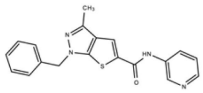	Z117416778	+	NA
Cc1nn(c2sc(cc12)C(=O)Nc1cccc(c1)S(=O)(=O)NCc1ccco1)C 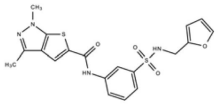	Z228719934	-	NA

Cc1nn(-c2ccccc2)c2sc(C(=O)Nc3ccc4c(c3)OCCO4)cc12 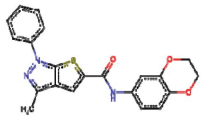	BCC0077119	+	+
O=C(Nc1ccccc1)c1ccc(S(=O)(=O)NCc2ccco2)cc1 	BCC0112913	-	NA
Cc1nn(-c2ccccc2)c2sc(C(=O)Nc3cccc(O)c3)cc12 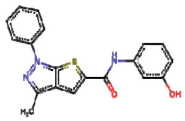	BCC0106222	++	-
CC(=O)c1cccc(NC(=O)c2cc3c(C)nn(-c4ccccc4)c3s2)c1	BCC0104214	+	NA
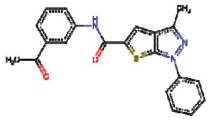			
Cc1c2cc(C(=O)NCc3ccco3)sc2nn1-c1ccccc1 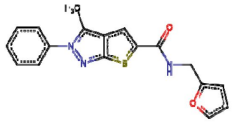	BCC0040387	-	NA
Cc1nn(-c2ccccc2)c2sc(C(=O)Nc3ccccc3Br)cc12 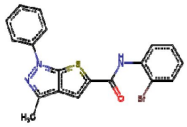	BCC0113320	+	+
Cc1nn(-c2ccccc2)c2sc(C(=O)Nc3nccs3)cc12 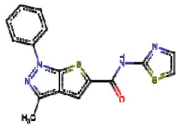	BCC0073142	-	NA
Cc1nn(-c2ccccc2)c2sc(C(=O)Nc3cccc(C(F)(F)F)c3)cc12	BCC0043997	-	NA

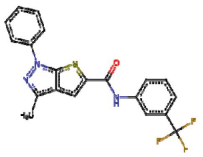			
Cc1nn(-c2ccccc2)c2sc(C(=O)Nc3ccccc3[N+](=O)[O-])cc12 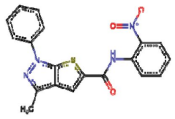	BCC0073242	-	NA
Cc1nn(-c2ccccc2)c(Cl)c1C(=O)NCc1ccco1 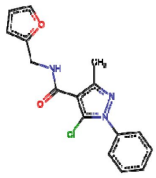	BCC0104192	-	NA
Cc1nn(-c2ccccc2)c2sc(C(=O)NN3C(=O)c4ccccc4C3=O)cc12 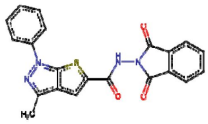	BCC0074259	-	NA
Structure of compound 21 analogue and fragment	**ID**	**ISR activation**	**GCN2 specificity**
CC(C)(CNC(=O)c1ccc(cc1)S(=O)(=O)C)c1ccc(cc1)Br 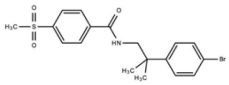	Z423087112	-	NA
Cc1ccc(cc1)-c1nnc([nH]1)NC(=O)c1cccc(c1)S(=O)(=O)C 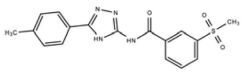	Z119766318	-	NA
COc1cc(cc(c1)-c1cnc2c(c(nn2c1)C)S(=O)(=O)N)OC 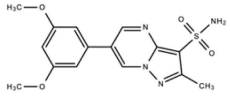	Z3464816516	-	NA
COc1ccc(cc1OC)-c1cnc2c(c(nn2c1)C)S(=O)(=O)N 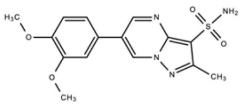	Z3464816527	-	NA
Structure of compound 20 analogue and fragment	**ID**	**ISR activation**	**GCN2 specificity**
Oc1ccc(c(c1)O)-c1csc(n1)Nc1ccccc1	Z48853885	-	NA

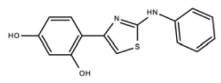			
COc1ccc(cc1)Nc1nc(cs1)-c1ccc(s1)CNC(=O)C 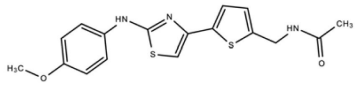	Z73485298	-	NA
CC(=O)NCc1ccc(s1)-c1csc(n1)Nc1ccc(cc1)F 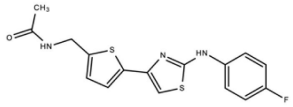	Z118606822	-	NA
CCOc1ccc(cc1)Nc1nc(cs1)-c1cnc(c1)C(=O)N1CCCC1 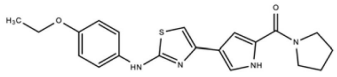	Z134826202	++	NA
FC(F)(F)c1ccccc1Nc1nc(cs1)-c1cnc(c1)C(=O)N1CCCC1 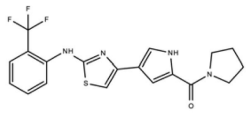	Z134826094	+	NA
COc1cccc(c1)Nc1nc(cs1)-c1cnc(c1)C(=O)N1CCCC1	Z134826982	++	NA
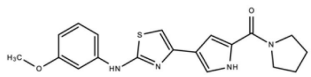			
Oc1ccc(c(c1)O)-c1csc(n1)Nc1ccccn1 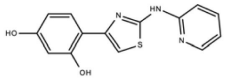	Z238766124	+	NA
COc1ccccc1Nc1nc(cs1)-c1ccc(o1)CNC(=O)C 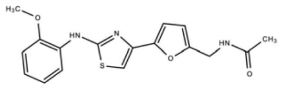	Z48856426	-	NA
CC(=O)NCc1ccc(o1)-c1csc(n1)Nc1cc(cc(c1)C)C 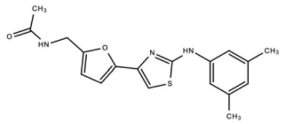	Z48859481	-	NA
CC(=O)NCc1ccc(o1)-c1csc(n1)Nc1ccc(c(c1)Cl)F 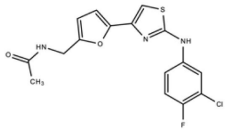	Z48857131	-	NA

COc1ccc(cc1)Nc1nc(cs1)-c1cc(n(c1C)-c1nnc[nH]1)C 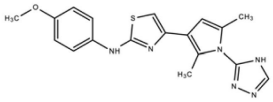	Z204017924	-	NA
Cc1cc(c(n1-c1nnc[nH]1)C)-c1csc(n1)Nc1ccccc1 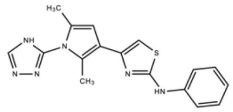	Z204003168	-	NA
CN1C(=C(C(=O)N(C)C1=O)c1csc(n1)Nc1ccc(cc1)F)N 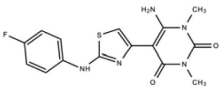	Z118606410	-	NA
CN1C(=C(C(=O)N(C)C1=O)c1csc(n1)Nc1ccccc1)N 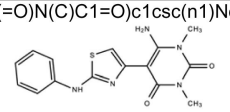	Z94733799	-	NA
Br.CC(=O)Nc1nc(c(s1)-c1csc(n1)Nc1ccccc1)C 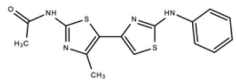	Z2854692688	-	NA
Br.CC(=O)Nc1nc(c(s1)-c1csc(n1)Nc1ccccn1)C	Z2239043599	-	NA
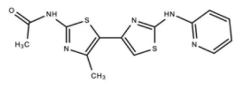			
Cc1cc(c(n1CC(F)(F)F)C)-c1csc(n1)Nc1ccccn1 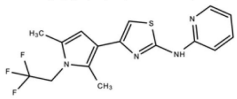	Z238766162	+	NA
Cl.Cc1cc(c([nH]1)C)-c1csc(n1)Nc1ccccn1 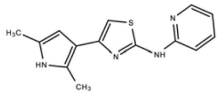	Z381026350	-	NA
Cl.Cc1cc(c(n1C1CC1)C)-c1csc(n1)Nc1ccccn1 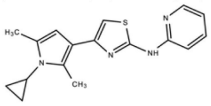	Z357935644	-	NA
Cl.Cc1cc(c(n1C)C)-c1csc(n1)Nc1ccccn1 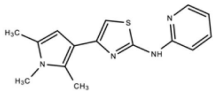	Z381543540	-	NA
Cc1nccc(n1)NCCCc1nc(cs1)-c1ccccn1	Z2582963583	-	NA

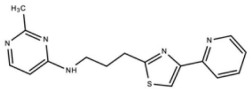			
Cc1nc(C)c(-c2csc(Nc3ncccn3)n2)s1 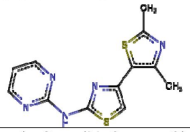	BCC0083926	-	NA
Oc1ccc(-c2csc(Nc3ncccn3)n2)cc1 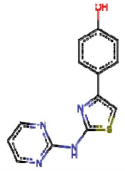	BCC0089540	+	+
Cc1nc(N)sc1-c1csc(Nc2ccc([N+](=O)[O-])cc2)n1 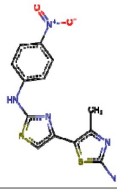	BCC0084097	++	-
Cc1cc(-c2csc(Nc3ncccn3)n2)ccc1F	BCC0080200	-	NA
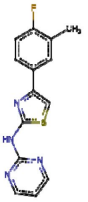			
CC(C)c1ccc(-c2csc(Nc3ncccn3)n2)cc1 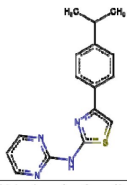	BCC0080152	-	NA
Cc1cccnc1Nc1nc(-c2sc(N)nc2C)cs1 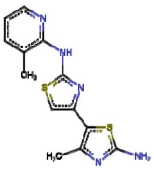	BCC0084738	+	+
Cc1cccc(Nc2nc(-c3sc(N)nc3C)cs2)n1	BCC0084842	-	NA

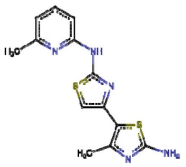			
Clc1ccc(-c2csc(Nc3ncccn3)n2)cc1 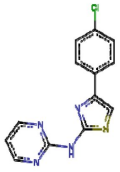	BCC0075509	-	NA
COc1ccc(-c2csc(Nc3ncccn3)n2)cc1 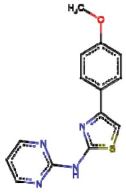	BCC0057431	-	NA
Cc1ccnc(Nc2nc(-c3sc(N)nc3C)cs2)c1	BCC0083923	+	+
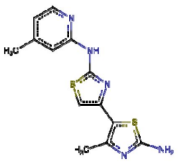			
Cc1nc(N)sc1-c1csc(Nc2cccnc2)n1 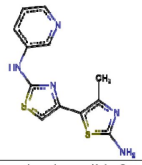	BCC0084758	-	NA
Cc1nc(N)sc1-c1csc(Nc2ccccc2F)n1 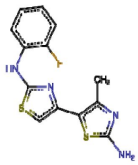	BCC0084762	+	-
Cc1nc(N)sc1-c1csc(Nc2cccc(O)c2)n1	BCC0105427	-	NA

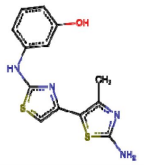			
Cc1ccc(C)c(Nc2nc(-c3sc(N)nc3C)cs2)c1 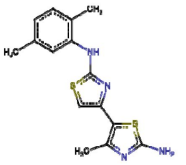	BCC0084833	-	NA
Cc1nc(N)sc1-c1csc(Nc2cccc(C(=O)O)c2)n1 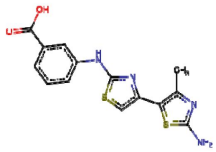	BCC0057014	-	NA
Cc1cc(O)ccc1Nc1nc(-c2sc(N)nc2C)cs1	BCC0084814	-	NA
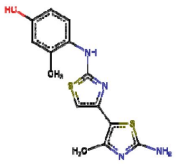			
CCOc1ccc(Nc2nc(-c3sc(N)nc3C)cs2)cc1 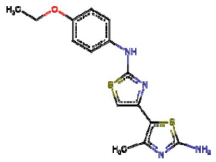	BCC0087543	+	-
Cc1nc(N)sc1-c1csc(Nc2ccccc2[N+](=O)[O-])n1 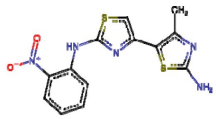	BCC0084744	-	NA
Cc1nc(C)c(-c2csc(Nc3ccccn3)n2)s1	BCC0079350	++	-
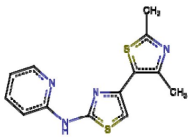			
Cc1nc(N)sc1-c1csc(NCCc2ccccc2)n1 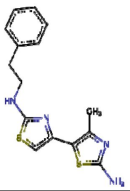	BCC0089615	-	NA
c1cnc(Nc2nc(-c3cccs3)cs2)nc1 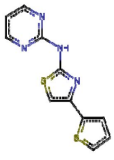	BCC0079876	-	NA
Cc1ccc(C)c(-c2csc(Nc3ncccn3)n2)c1	BCC0080199	-	NA

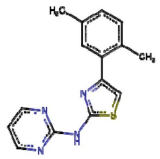			
Cc1nc(N)sc1-c1csc(N/N=C/c2cccnc2)n1 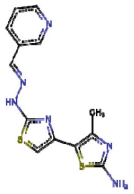	BCC0041121	-	NA
Cc1nc(N)sc1-c1csc(Nc2ccc(O)c(C(=O)O)c2)n1 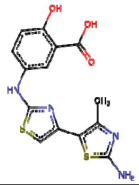	BCC0089519	-	NA
Fc1ccc(-c2csc(Nc3ncccn3)n2)cc1	BCC0084830	-	NA
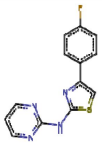			
Cc1cc(C)nc(NS(=O)(=O)c2ccc(Nc3nc(-c4sc(N)nc4C)cs3)cc2)n1 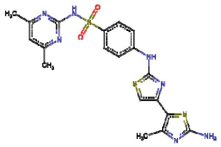	BCC0087668	-	NA

NA = not applicable; assay not performed due to the inactivity of the analogue c

Data availability

Raw data are available on reasonable request.

Acknowledgements

SJM was supported by the MRC (G1002610, MR/V028669/1 and MR/R009120/1), EPSRC (EP/R03558X/1), Cambridge Biomedical Research Centre (BRC-1215-20014); British Lung Foundation, Asthma+Lung UK, Royal Papworth Hospital, Alpha1 Foundation. GE was supported by philanthropic funding from Rick Medlock and by awards from EPSRC (EP/R03558X/1), BHF (RE/18/1/34212), Evelyn Trust (Grant 22/03), and the Cambridge-Tsinghua collaborative programme on sustainability and emerging technologies. JZ was supported by the Doctoral Training Programme in Medical Research (DTP-MR; Cambridge Trust). GRM is supported by a Baxter Fellowship from the University of Dundee, and a TENOVUS grant T21/01 119615, and Biotechnology and Biological Sciences Research Council (UKRI-BBSRC) Capital Equipment Grant BB/V019635/1. VV supported by MRC iCase Studentship (MR/R01579/1). This research was supported by the CIMR Flow Cytometry Core Facility. We wish to thank Reiner Schulte and Gabriela Grondys-Kotarba for their advice and support in flow cytometry cell sorting. We wish to thank Heather Harding for helpful discussions and reagents. We wish to thank Steve Andrews, Kushal Rugjee, and other colleagues at the ADDI for help with chemical library preparation. Thanks to Apollo Therapeutics Ltd for conducting the LanthaScreen in vitro kinase activity at Selvita S.A, Krakow, Poland.

Additional files

Supplementary Figure 1 Kinetics of responses to compounds 20 and 21. (A-B) Wild-type CHO cells stably expressing the ATF4::nanoLuc-PEST reporter were treated with Nano-Glo and either (A) 13μM compound 20 or (B) 13μM compound 21. Median bioluminescence (fold change normalised to DMSO control) ± 95% confidence. Representative experiment (n=4 technical repeats). (C-F) Representative immunoblot of lysates from wild-type or *Eif2ak4*$^{-/-}$CHO cells treated with 10μM compound 20 or 7.5μM 21 for the indicated times. Immediately before harvesting, cells were treated with 10μg/mL puromycin to label newly synthesised polypeptides. "-" indicates cells not incubated with puromycin. "U" cells were treated with puromycin but without test compound. "CHX" represents the cycloheximide control (100μg/mL). Molecular size in kDa. (E-F) Quantification of puromycinylated proteins normalised to GAPDH. Mean ± SEM. CHO WT (black) and *Eif2ak4*$^{-/-}$ cells (turquoise. N = 4 independent experiments. Two-way ANOVA with Šídák's multiple comparisons test; ***: $p \leq 0.001$.

Supplementary Figure 2 Cell-type differences in response to histidinol. Fold-change of ATF4::NanoLuc reporter signal in HEK293T, HeLa and CHO cells transiently transfected with reporter and treated for 20 hours with 3mM histidinol. Fold-change calculated relative to vehicle control. Mean ± SEM.

Supplementary Figure 3 GCN2-dependence of ISR activation by putative GCN2 agonists. Normalised fold-change in ATF4 signal in CHO WT (purple) and Gcn2-/- (blue) ATF4::NanoLuc reporter cells treated for 19 hours with a panel of ATP-competitive kinase inhibitors reported to activate GCN2 (at 1 and 3μM, sunitinib used at 3 and 10μM, AZD1175 used at 0.3 and 1μM, gefitinib and erlotinib used at 3 and 10μM). DMSO was used as vehicle control. (n=3; mean ± SEM).

Additional information

Funding

Funder	Grant reference number	Author
Cambridge Trust (Cambridge Commonwealth, European & International Trust)		JiaYi Zhu

University of Cambridge		JiaYi Zhu
Medical Research Council	G1002610	Stefan J Marciniak
Medical Research Council	MR/V028669/1	Stefan J Marciniak
Medical Research Council	MR/R009120/1	Stefan J Marciniak

Author ORCID iDs

JiaYi Zhu: https://orcid.org/0000-0001-7401-6468
Giulia Emanuelli: https://orcid.org/0000-0001-8899-6110
Glenn R Masson: https://orcid.org/0000-0002-1386-4719
Henriette Willems: https://orcid.org/0000-0001-7196-5975
Joseph E Chambers: https://orcid.org/0000-0003-4675-0053
Stefan J Marciniak: https://orcid.org/0000-0001-8472-7183

References

1. **Harding HP,** Zhang Y, Zeng H, Novoa I, Lu PD, Calfon M, et al. (2003) An integrated stress response regulates amino acid metabolism and resistance to oxidative stress. *Mol Cell* **11**:619-33 https://doi.org/10.1016/s1097-2765(03)00105-9 | PubMed
2. **Emanuelli G,** Nassehzadeh-Tabriz N, Morrell NW, Marciniak SJ (2020) The integrated stress response in pulmonary disease. *Eur Respir Rev* **29**:200184 https://doi.org/10.1183/16000617.0184-2020 | PubMed
3. **Gupta R,** Hinnebusch AG (2023) Differential requirements for P stalk components in activating yeast protein kinase Gcn2 by stalled ribosomes during stress. *Proc Natl Acad Sci U S A* **120**:e2300521120 https://doi.org/10.1073/pnas.2300521120 | PubMed
4. **Wu CC,** Peterson A, Zinshteyn B, Regot S, Green R (2020) Ribosome Collisions Trigger General Stress Responses to Regulate Cell Fate. *Cell* **182**:404-16. https://doi.org/10.1016/j.cell.2020.06.006 | PubMed
5. **Wu Y,** Yang Y, Qin X, Zhang Z, Ullah M, Li Y, et al. (2024) Unfolded proteins in the mitochondria activate HRI and inhibit mitochondrial protein translation. *Cell Signal* **123** https://doi.org/10.1016/j.cellsig.2024.111353 | PubMed
6. **Zhu S,** Nguyen A, Pang J, Zhao J, Chen Z, Liang Z, et al. (2022) Mitochondrial Stress Induces an HRI-eIF2alpha Pathway Protective for Cardiomyopathy. *Circulation* **146**:1028-31 https://doi.org/10.1161/circulationaha.122.059594 | PubMed
7. **Chakrabarty Y,** Yang Z, Chen H, Chan DC (2024) The HRI branch of the integrated stress response selectively triggers mitophagy. *Mol Cell* **84**:1090-100. https://doi.org/10.1016/j.molcel.2024.01.016 | PubMed
8. **Marciniak SJ,** Chambers JE, Ron D (2021) Pharmacological targeting of endoplasmic reticulum stress in disease. *Nat Rev Drug Discov* https://doi.org/10.1038/s41573-021-00320-3 | PubMed
9. **Carlson KR,** Georgiadis MM, Tameire F, Staschke KA, Wek RC (2023) Activation of Gcn2 by small molecules designed to be inhibitors. *J Biol Chem* **299**:104595 https://doi.org/10.1016/j.jbc.2023.104595 | PubMed
10. **Fujimoto J,** Kurasawa O, Takagi T, Liu X, Banno H, Kojima T, et al. (2019) Identification of Novel, Potent, and Orally Available GCN2 Inhibitors with Type I Half Binding Mode. *ACS Med Chem Lett* **10**:1498-503 https://doi.org/10.1021/acsmedchemlett.9b00400 | PubMed
11. **Szaruga M,** Janssen DA, de Miguel C, Hodgson G, Fatalska A, Pitera AP, et al. (2023) Activation of the integrated stress response by inhibitors of its kinases. *Nature communications* **14**:5535 https://doi.org/10.1038/s41467-023-40823-8 | PubMed
12. **Hinnebusch AG,** Lorsch JR (2012) The mechanism of eukaryotic translation initiation: new insights and challenges. *Cold Spring Harb Perspect Biol* **4**:a011544 https://doi.org/10.1101/cshperspect.a011544 | PubMed

13. **Matts RL,** Levin DH, London IM (1983) Effect of phosphorylation of the alpha-subunit of eukaryotic initiation factor 2 on the function of reversing factor in the initiation of protein synthesis. *Proc Natl Acad Sci U S A* **80**:2559-63 https://doi.org/10.1073/pnas.80.9.2559 | PubMed

14. **Lu PD,** Harding HP, Ron D (2004) Translation reinitiation at alternative open reading frames regulates gene expression in an integrated stress response. *J Cell Biol* **167**:27-33 https://doi.org/10.1083/jcb.200408003 | PubMed

15. **Novoa I,** Zeng H, Harding HP, Ron D (2001) Feedback inhibition of the unfolded protein response by GADD34-mediated dephosphorylation of eIF2alpha. *J Cell Biol* **153**:1011-22 https://doi.org/10.1083/jcb.153.5.1011 | PubMed

16. **Marciniak SJ,** Yun CY, Oyadomari S, Novoa I, Zhang Y, Jungreis R, et al. (2004) CHOP induces death by promoting protein synthesis and oxidation in the stressed endoplasmic reticulum. *Genes Dev* **18**:3066-77 https://doi.org/10.1101/gad.1250704 | PubMed

17. **Emanuelli G,** Zhu J, Li W, Morrell NW, Marciniak SJ (2024) Functional validation of EIF2AK4 (GCN2) missense variants associated with pulmonary arterial hypertension. *Hum Mol Genet* **33**:1495-505 https://doi.org/10.1093/hmg/ddae082 | PubMed

18. **Masson GR** (2019) Towards a model of GCN2 activation. *Biochem Soc Trans* **47**:1481-8 https://doi.org/10.1042/bst20190331 | PubMed

19. **Garcia-Barrio M,** Dong J, Ufano S, Hinnebusch AG (2000) Association of GCN1-GCN20 regulatory complex with the N-terminus of eIF2alpha kinase GCN2 is required for GCN2 activation. *EMBO J* **19**:1887-99 https://doi.org/10.1093/emboj/19.8.1887 | PubMed

20. **Kubota H,** Sakaki Y, Ito T (2000) GI domain-mediated association of the eukaryotic initiation factor 2alpha kinase GCN2 with its activator GCN1 is required for general amino acid control in budding yeast. *J Biol Chem* **275**:20243-6 https://doi.org/10.1074/jbc.c000262200 | PubMed

21. **Sattlegger E,** Hinnebusch AG (2000) Separate domains in GCN1 for binding protein kinase GCN2 and ribosomes are required for GCN2 activation in amino acid-starved cells. *EMBO J* **19**:6622-33 https://doi.org/10.1093/emboj/19.23.6622 | PubMed

22. **Wek SA,** Zhu S, Wek RC (1995) The histidyl-tRNA synthetase-related sequence in the eIF-2 alpha protein kinase GCN2 interacts with tRNA and is required for activation in response to starvation for different amino acids. *Mol Cell Biol* **15**:4497-506 https://doi.org/10.1128/mcb.15.8.4497 | PubMed

23. **Dong J,** Qiu H, Garcia-Barrio M, Anderson J, Hinnebusch AG (2000) Uncharged tRNA activates GCN2 by displacing the protein kinase moiety from a bipartite tRNA-binding domain. *Mol Cell* **6**:269-79 https://doi.org/10.1016/s1097-2765(00)00028-9 | PubMed

24. **Harding HP,** Ordonez A, Allen F, Parts L, Inglis AJ, Williams RL, et al. (2019) The ribosomal P-stalk couples amino acid starvation to GCN2 activation in mammalian cells. *eLife* **8**:e50149 https://doi.org/10.7554/eLife.50149 | PubMed

25. **Inglis AJ,** Masson GR, Shao S, Perisic O, McLaughlin SH, Hegde RS, et al. (2019) Activation of GCN2 by the ribosomal P-stalk. *Proc Natl Acad Sci U S A* **116**:4946-54 https://doi.org/10.1073/pnas.1813352116 | PubMed

26. **Tang CP,** Clark O, Ferrarone JR, Campos C, Lalani AS, Chodera JD, et al. (2022) GCN2 kinase activation by ATP-competitive kinase inhibitors. *Nat Chem Biol* **18**:207-15 https://doi.org/10.1038/s41589-021-00947-8 | PubMed

27. **Roskoski R Jr** (2016) Classification of small molecule protein kinase inhibitors based upon the structures of their drug-enzyme complexes. *Pharmacol Res* **103**:26-48 https://doi.org/10.1016/j.phrs.2015.10.021 | PubMed

28. **Neill G,** Vinciauskaite V, Paul M, Gilley R, Cook SJ, Masson GR (2024) Paradoxical Activation of GCN2 by ATP-competitive inhibitors via allosteric activation and autophosphorylation. *bioRxiv* https://doi.org/10.1101/2024.08.14.606984

29. **Drainas AP,** Hsu WH, Dallas AE, Poltorack CD, Kim JW, He A, et al. (2024) GCN2 is a determinant of the response to WEE1 kinase inhibition in small-cell lung cancer. *Cell Rep* **43**:114606 https://doi.org/10.1016/j.celrep.2024.114606 | PubMed

30. **Tjeerdsma RB,** Ng TF, Roorda M, Bianchi D, Yang S, Bonnet C, et al. (2025) WEE1 inhibitors trigger GCN2-mediated activation of the integrated stress response. *bioRxiv* https://doi.org/10.1101/2025.03.12.642754

31. **Wilson JCJ,** Zhu J, Lam S, Hart A, Goh CG, Bou-Dagher F, et al. (2025) WEE1 inhibitors synergise with mRNA translation defects via activation of the kinase GCN2. *bioRxiv* https://doi.org/10.1101/2025.03.12.642825

32. **Solorio-Kirpichyan K,** Fan X, Golovenko D, Korostelev AA, Yan N, Korennykh A (2024) Cryo-EM structure of histidyl-tRNA synthetase-like domain reveals activating crossed helices at the core of GCN2. *PNAS Nexus* **3** https://doi.org/10.1093/pnasnexus/pgae528 | PubMed

33. **Bou-Nader C,** Gaikwad S, Bahmanjah S, Zhang F, Hinnebusch AG, Zhang J (2024) Gcn2 structurally mimics and functionally repurposes the HisRS enzyme for the integrated stress response. *Proc Natl Acad Sci U S A* **121**:e2409628121 https://doi.org/10.1073/pnas.2409628121 | PubMed

34. **Yin JZ,** Keszei AFA, Houliston S, Filandr F, Beenstock J, Daou S, et al. (2024) The HisRS-like domain of GCN2 is a pseudoenzyme that can bind uncharged tRNA. *Structure* **32**:795-811. https://doi.org/10.1016/j.str.2024.02.021 | PubMed

35. **Grummt F,** Grummt I (1976) Studies on the role of uncharged tRNA in pleiotypic response of animal cells. *Eur J Biochem* **64**:307-12 https://doi.org/10.1111/j.1432-1033.1976.tb10302.x | PubMed

36. **Oliveira MM,** Mohamed M, Elder MK, Banegas-Morales K, Mamcarz M, Lu EH, et al. (2024) The integrated stress response effector GADD34 is repurposed by neurons to promote stimulus-induced translation. *Cell Rep* **43**:113670 https://doi.org/10.1016/j.celrep.2023.113670 | PubMed

37. **Chambers JE,** Dalton LE, Clarke HJ, Malzer E, Dominicus CS, Patel V, et al. (2015) Actin dynamics tune the integrated stress response by regulating eukaryotic initiation factor 2alpha dephosphorylation. *eLife* **4** https://doi.org/10.7554/eLife.04872 | PubMed

38. **Harding HP,** Zhang Y, Ron D (1999) Protein translation and folding are coupled by an endoplasmic-reticulum-resident kinase. *Nature* **397**:271-4 https://doi.org/10.1038/16729 | PubMed

39. **Sekine Y,** Zyryanova A, Crespillo-Casado A, Amin-Wetzel N, Harding HP, Ron D (2016) Paradoxical Sensitivity to an Integrated Stress Response Blocking Mutation in Vanishing White Matter Cells. *PLoS One* **11**:e0166278 https://doi.org/10.1371/journal.pone.0166278 | PubMed

40. **Guo L,** Shao W, Zhou C, Yang H, Yang L, Cai Q, et al. (2023) Neratinib for HER2-positive breast cancer with an overlooked option. *Mol Med* **29**:134 https://doi.org/10.1186/s10020-023-00736-0 | PubMed

41. **Pochopien AA,** Beckert B, Kasvandik S, Berninghausen O, Beckmann R, Tenson T, et al. (2021) Structure of Gcn1 bound to stalled and colliding 80S ribosomes. *Proc Natl Acad Sci U S A* **118**:e2022756118 https://doi.org/10.1073/pnas.2022756118 | PubMed

42. **Hansen BS,** Vaughan MH, Wang L (1972) Reversible inhibition by histidinol of protein synthesis in human cells at the activation of histidine. *J Biol Chem* **247**:3854-7 https://doi.org/10.1016/s0021-9258(19)45112-0 | PubMed

43. **Snieckute G,** Genzor AV, Vind AC, Ryder L, Stoneley M, Chamois S, et al. (2022) Ribosome stalling is a signal for metabolic regulation by the ribotoxic stress response. *Cell Metab* **34**:2036-46. https://doi.org/10.1016/j.cmet.2022.10.011 | PubMed

44. **Gilley R,** Kidger AM, Neill G, Severson P, Byrne DP, Kenneth NS, et al. (2024) RAF inhibitors activate the integrated stress response by direct activation of GCN2. *bioRxiv* https://doi.org/10.1101/2024.08.15.607884

45. **Pacey S,** Leung C, Rodney S, DosReis AFP, Ruddle R, Tall M, et al. (2024) Abstract CT111: Pharmacokinetic and pharmacodynamic evaluation of NXP800, a novel GCN2 activator, in a first in human clinical trial. *Cancer Research* **84**:CT111-CT https://doi.org/10.1158/1538-7445.am2024-ct111

46. **Ill CR,** Marikar NC, Nguyen V, Nangia V, Darnell AM, Vander Heiden MG, et al. (2024) BRAF(V600) and ErbB inhibitors directly activate GCN2 in an off-target manner to limit cancer cell proliferation. *bioRxiv* https://doi.org/10.1101/2024.12.19.629301 | PubMed

47. **Robers MB,** Wilkinson JM, Vasta JD, Berger LM, Berger BT, Knapp S (2021) Single tracer-based protocol for broad-spectrum kinase profiling in live cells with NanoBRET. *STAR Protoc* **2**:100822 https://doi.org/10.1016/j.xpro.2021.100822 | PubMed

48. **Marciniak SJ,** Garcia-Bonilla L, Hu J, Harding HP, Ron D (2006) Activation-dependent substrate recruitment by the eukaryotic translation initiation factor 2 kinase PERK. *J Cell Biol* **172**:201-9 https://doi.org/10.1083/jcb.200508099 | PubMed

49. **Dalton LE,** Healey E, Irving J, Marciniak SJ (2012) Phosphoproteins in stress-induced disease. *Prog Mol Biol Transl Sci* **106**:189-221 https://doi.org/10.1016/b978-0-12-396456-4.00003-1 | PubMed

50. **Jadhav M,** Sankhe K, Bhandare RR, Edis Z, Bloukh SH, Khan TA (2021) Synthetic Strategies of Pyrimidine-Based Scaffolds as Aurora Kinase and Polo-like Kinase Inhibitors. *Molecules* **26** https://doi.org/10.3390/molecules26175170 | PubMed

51. **Lough L,** Sherman D, Beccera-Flores M, Lavinda O, Ni E, Wang H, et al. (2018) Triazolo[4,5-d]pyrimidines as Validated General Control Nonderepressible 2 (GCN2) Protein Kinase Inhibitors Reduce Growth of Leukemia Cells. *Comput Struct Biotechnol J* **16**:350-60 https://doi.org/10.1016/j.csbj.2018.09.003 | PubMed

52. **Berlanga JJ,** Ventoso I, Harding HP, Deng J, Ron D, Sonenberg N, et al. (2006) Antiviral effect of the mammalian translation initiation factor 2alpha kinase GCN2 against RNA viruses. *EMBO J* **25**:1730-40 https://doi.org/10.1038/sj.emboj.7601073 | PubMed

53. **Krishnamoorthy J,** Mounir Z, Raven JF, Koromilas AE (2008) The eIF2alpha kinases inhibit vesicular stomatitis virus replication independently of eIF2alpha phosphorylation. *Cell Cycle* **7**:2346-51 https://doi.org/10.4161/cc.6323 | PubMed

54. **Sattlegger E,** Hinnebusch AG (2005) Polyribosome binding by GCN1 is required for full activation of eukaryotic translation initiation factor 2alpha kinase GCN2 during amino acid starvation. *J Biol Chem* **280**:16514-21 https://doi.org/10.1074/jbc.m414566200 | PubMed

55. **Marton MJ,** Crouch D, Hinnebusch AG (1993) GCN1, a translational activator of GCN4 in Saccharomyces cerevisiae, is required for phosphorylation of eukaryotic translation initiation factor 2 by protein kinase GCN2. *Mol Cell Biol* **13**:3541-56 https://doi.org/10.1128/mcb.13.6.3541-3556.1993 | PubMed

56. **Hinnebusch AG** (1985) A hierarchy of trans-acting factors modulates translation of an activator of amino acid biosynthetic genes in Saccharomyces cerevisiae. *Mol Cell Biol* **5**:2349-60 https://doi.org/10.1128/mcb.5.9.2349-2360.1985 | PubMed

57. **Anda S,** Zach R, Grallert B (2017) Activation of Gcn2 in response to different stresses. *PLoS One* **12**:e0182143 https://doi.org/10.1371/journal.pone.0182143 | PubMed

58. **Das D,** Sikdar P, Bairagi M (2016) Recent developments of 2-aminothiazoles in medicinal chemistry. *Eur J Med Chem* **109**:89-98 https://doi.org/10.1016/j.ejmech.2015.12.022 | PubMed

59. **Jakopin Z** (2020) 2-aminothiazoles in drug discovery: Privileged structures or toxicophores?. *Chem Biol Interact* **330**:109244 https://doi.org/10.1016/j.cbi.2020.109244 | PubMed

60. **Devine SM,** Mulcair MD, Debono CO, Leung EW, Nissink JW, Lim SS, et al. (2015) Promiscuous 2-aminothiazoles (PrATs): a frequent hitting scaffold. *Journal of medicinal chemistry* **58**:1205-14 https://doi.org/10.1021/jm501402x | PubMed

61. **Ben-David U,** Siranosian B, Ha G, Tang H, Oren Y, Hinohara K, et al. (2018) Genetic and transcriptional evolution alters cancer cell line drug response. *Nature* **560**:325-30 https://doi.org/10.1038/s41586-018-0409-3 | PubMed

62. **de Oliveira T Maia,** Korboukh V, Caswell S, Winter Holt JJ, Lamb M, Hird AW, et al. (2020) The structure of human GCN2 reveals a parallel, back-to-back kinase dimer with a plastic DFG activation loop motif. *Biochem J* **477**:275-84 https://doi.org/10.1042/bcj20190196 | PubMed

63. **Sastry GM,** Adzhigirey M, Day T, Annabhimoju R, Sherman W (2013) Protein and ligand preparation: parameters, protocols, and influence on virtual screening enrichments. *J Comput Aided Mol Des* **27**:221-34 https://doi.org/10.1007/s10822-013-9644-8 | PubMed

Peer reviews

Reviewer #1 (Public review):

Summary:

This manuscript describes a chemical screen for activators of the eIF2 kinase GCN2 (EIF2AK4) in the integrated stress response (ISR). Recently, reported inhibitors of GCN2 and other protein kinases have been shown at certain concentrations to paradoxically activate GCN2. The study uses CHO cells and ISR reporter screens to identify a number of GCN2 activator compounds, including a potent "compound 20." These activators have implications for the development of new therapies for ISR-related diseases. For example, although not directly pursued in this study, these GCN2 activators could be helpful for the treatment of PVOD, which is reported for patients with certain GCN2 loss-of-function mutations. The identified activators are also suggested to engage with the GCN2 directly and can function devoid of GCN1, a co-activator of GCN2.

Strengths:

The manuscript appears to be a largely rigorous study that flows in a logical manner. The topic is interesting and significant.

Weaknesses:

Portions of the manuscript are not fully clear. There are some experimental presentation and design concerns that should be addressed to support the stated conclusions.

https://doi.org/10.7554/eLife.108590.2.sa3

Reviewer #2 (Public review):

Summary:

In this manuscript Zhu, Emanuelli and colleagues describe a novel pharmacological activator of the Integrated Stress Response kinase GCN2. The work is conclusive and biochemically solid. This work significantly adds to the pharmacological arsenal targeting the ISR and in particular GCN2.

Strengths:

Strong biochemistry, novel molecular activator of GCN2 (GCN1 independent).

Weaknesses:

Rationale for the screen not exploited in the results (e.g. pathogenic GCN2 mutants), lots of cell-based read-outs not endogenous.

Comments on revised version.

The authors did a great job at addressing my initial critique on their manuscript and consequently I have no further comment.

https://doi.org/10.7554/eLife.108590.2.sa2

Reviewer #3 (Public review):

Summary:

In this manuscript, the authors describe the results of a high throughput screen for small molecule activators of GCN2. Ultimately, they find 3 promising compounds. One of these three, compound 20 (C20) is of the most interest both for its potency and specificity. The major new finding is that this molecule appears to activate GCN2 independent of GCN1, which suggests that it works by a potentially novel mechanism. Biochemical analysis suggests that each bind in the ATP binding pocket of GCN2, and that at least in vitro C20 is a potent agonist. Structural modeling provides insight into how the three compounds might dock in the pocket and generates testable hypotheses as to why C20 perhaps acts through a different mechanism than other molecules.

Strengths:

Of the 3 compounds identified by the authors, C20 is of the most interest, not just for its intriguing mechanistic distinction as being GCN1-independent (shown genetically in two distinct cell lines, CHO and 293T, and in contrast to other GCN2 activators) but also for its potency. Ultimately, C20 might be a tool for providing mechanistic insight into the details of GCN2 activation and regulation and could be exploited therapeutically.

Weaknesses:

The chief limitation of this work is that the experiments exploring the effects of C20 on ISR output in cells are limited, so how useful these compounds are both experimentally and therapeutically remains to be determined.

Comments on revised version.

The authors have satisfactorily addressed my comments. A more extensive analysis of UPR signaling in cells (transcription and cell death in particular) would have further strengthened the paper, but that can be left to future work.

https://doi.org/10.7554/eLife.108590.2.sa1

Author response:

The following is the authors' response to the original reviews

> ***Public Reviews:***
>
> ***Reviewer #1 (Public review):***
>
> *Summary:*
>
> *This manuscript describes a chemical screen for activators of the eIF2 kinase GCN2 (EIF2AK4) in the integrated stress response (ISR). Recently, reported inhibitors of GCN2 and other protein kinases have been shown at certain concentrations to paradoxically activate GCN2. The study uses CHO cells and ISR reporter screens to identify a number of GCN2 activator compounds, including a potent "compound 20." These activators have implications for the development of new therapies for ISR-related diseases. For example, although not directly pursued in this study, these GCN2 activators could be helpful for the treatment of PVOD, which is reported for patients with certain GCN2 loss-of-function mutations. The identified activators are also suggested to engage with the GCN2 directly and can function while devoid of GCN1, a co-activator of GCN2.*

> *Strengths:*
>
> *The manuscript appears to be a largely rigorous study that flows in a logical manner. The topic is interesting and significant.*
>
> *Weaknesses:*
>
> *Portions of the manuscript are not fully clear. Some experimental presentation and design concerns should be addressed to support the stated conclusions.*

We thank the reviewer for their supportive comments. We agree that portions of the manuscript were not fully clear and that some aspects of the experimental presentation and design required clarification.

To address this, we have revised the manuscript to make the experimental logic more transparent. In particular, we now explain more clearly the rationale for the screening strategy, including the use of histidinol as a canonical GCN2 activator, latrunculin A as a modulator of PPP1R15A-mediated eIF2α dephosphorylation, and tunicamycin as a PERK-dependent ER-stress control. We also clarify why a submaximal concentration of histidinol was used: this was intended to reveal compounds that enhance ISR signalling when GCN2 is partially activated.

We have clarified the use of the two ATF4 reporter systems. The ATF4–NanoLuc reporter was used for sensitive primary screening, whereas the ATF4–luc2 reporter was used as a more stringent orthogonal assay to prioritise robust ISR activators. We now state explicitly why some initial hits were not retained after testing in the second reporter line, and why the NanoLuc system was subsequently used again for mechanistic experiments.

Finally, we have revised the presentation of the orthogonal validation steps to make clearer how they support the stated conclusions. These include assays designed to distinguish GCN2-dependent ISR activation from indirect activation through ER stress, additional analysis of GCN2 dependence, and clearer interpretation of biochemical and docking data.

We hope that these revisions address the reviewer's concern that the experimental design and data presentation needed to be made clearer in order to support the conclusions.

> ***Reviewer #2 (Public review):***
>
> *Summary:*
>
> *In this manuscript, Zhu, Emanuelli, and colleagues describe a novel pharmacological activator of the Integrated Stress Response kinase GCN2. The work is conclusive and biochemically solid. This work significantly adds to the pharmacological arsenal targeting the ISR and, in particular, GCN2.*
>
> *Strengths:*
>
> *Strong biochemistry, novel molecular activator of GCN2 (GCN1 independent).*
>
> *Weaknesses:*
>
> *The rationale for the screen is not exploited in the results (e.g., pathogenic GCN2 mutants), and lots of cell-based read-outs are not endogenous.*

We thank this reviewer for their positive assessment of the work. We address the three major concerns in turn below.

> *Major points*

> *(1) Regarding the justification of the work. Since the authors justify the screen for GCN2 activators with loss-of-function mutants associated with diseases, it would be of interest to evaluate whether the best compounds identified in the study are indeed able to prompt activation of those mutants (or at least of the most prevalent). This approach could actually go in parallel with the docking experiments carried out in the last figure of the manuscript, where mutants could be modelized as well.*

To address this point, we tested whether the lead compounds could activate disease-associated GCN2 variants linked to pulmonary veno-occlusive disease. In contrast to GCN2iB, the new compounds did not activate these variants. We now state this explicitly in the manuscript, thereby clarifying that although the compounds identify a new mode of GCN2 activation, they do not rescue the pathogenic GCN2 variants tested here.

Results

"Moreover, in contrast to GCN2iB (17), the current compounds did not activate disease-associated GCN2 variants linked to PVOD [data not shown]."

> *(2) The compounds are only tested using « artificial » proximal signaling outputs. It would be interesting to evaluate whether the best identified compounds are capable of prompting endogenous eIF2alpha phosphorylation in cellular models.*

We thank the reviewer for this suggestion. Detecting eIF2α phosphorylation following activation of GCN2 is technically challenging and typically produces weaker signals compared to activation of other ISR kinases, such as PERK (e.g. by thapsigargin). For this reason, many studies rely on downstream reporter assays to monitor GCN2 activity. To address the reviewer's concern, we have now included an orthogonal readout of ISR activation by assessing global translation using a puromycin incorporation assay. Using this approach, we show that compound 20 significantly reduces translation, and importantly, this effect is attenuated in GCN2-deficient cells, supporting a GCN2-dependent mechanism.

Results

"Studies with compound 18 were limited by poor aqueous solubility; therefore, time-course analyses focused on compounds 20 and 21. To assess ISR activation over an extended period, live-cell luciferase measurements were performed using CHO cells stably expressing an ATF4::Nanoluc-PEST reporter. Both compounds elicited maximal reporter activation between 6 and 8 h (Figure S1A&B). Compound 20, but not 21, induced a significant GCN2-dependent reduction in mRNA translation, as measured by puromycin incorporation, with a progressive effect observed up to 7 h (Figure S1C-F)."

> *(3) Other GCN2 activators (other than GCN2iB, e.g., HC-7366) were recently identified. In this context, it would be of interest to carry out a small benchmarking study to evaluate how the compounds identified in the current study perform against the previously identified molecules.*

We thank the reviewer for this suggestion. In response, we obtained HC-7366 and assessed its activity alongside our compounds in the CHO ATF4::NanoLuc reporter assay. In this system, compound 20 demonstrated greater potency than HC-7366 (see reviewer figure below). However, we note that HC-7366 showed relatively limited activity in CHO cells in our hands, despite previously reported strong effects in other cellular systems and in vivo models. This context-dependent activity makes direct benchmarking difficult. Accordingly, we have included this comparison in the revised manuscript and discuss this limitation in the Discussion.

Discussion

"We also evaluated the reported GCN2 activator HC-7366 in our CHO ATF4::NanoLuc reporter system. In this context, HC-7366 showed limited activity relative to compound 20, despite its reported efficacy in other cellular systems and in vivo (data not shown). This highlights potential context dependence in small-molecule activation of GCN2 and limits direct cross-study comparison."

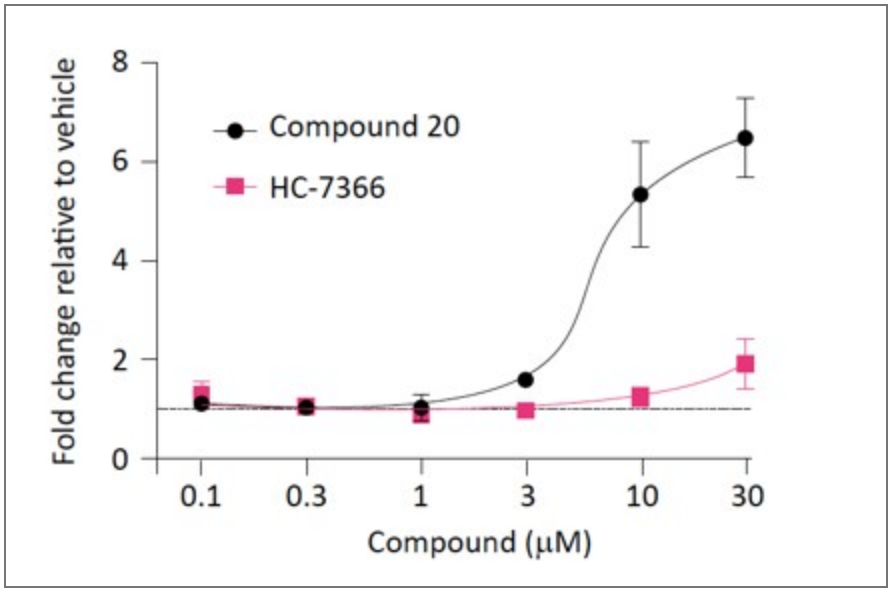

Author response image 1. ISR activation by compound 20 and GC-7366 in CHO cells Normalised fold-change in ATF4 signal in CHO ATF4::NanoLuc reporter cells treated for 19 hours with Compound 20 or HC-7366. DMSO was used as vehicle control. (representative experiment, mean ± SEM, n=3 technical replicates).

> ***Reviewer #3 (Public review):***
>
> *Summary:*
>
> *In this manuscript, the authors describe the results of a high-throughput screen for small-molecule activators of GCN2. Ultimately, they find 3 promising compounds. One of these three, compound 20 (C20), is of the most interest both for its potency and specificity. The major new finding is that this molecule appears to activate GCN2 independent of GCN1, which suggests that it works by a potentially novel mechanism. Biochemical analysis suggests that each binds in the ATP-binding pocket of GCN2, and that at least in vitro, C20 is a potent agonist. Structural modeling provides insight into how the three compounds might dock in the pocket and generates testable hypotheses as to why C20 perhaps acts through a different mechanism than other molecules.*

We agree that GCN1-independent activation suggests a potentially distinct mechanism of action. While we are currently unable to define the mechanistic basis underlying the GCN1-independence of compound 20, prior work provides some relevant context. Recent studies have shown that the ATP-competitive modulator GCN2iB can activate GCN2 independently of GCN1 under specific conditions, notably in the context of the GCN2 E26A mutant [Carlson, 2023]. This observation raises the possibility that, under certain conditions, engagement of the kinase domain, potentially via the ATP-binding pocket, may bypass the requirement for GCN1. However, in our system, we did not observe GCN1-independent activation with

B at the concentrations tested. This discrepancy may reflect a narrow or context-dependent window for such activity, or differences between wild-type and mutant GCN2. These findings suggest that GCN1-independent activation of GCN2 may occur under specific conditions or with distinct classes of compounds, although further work will be required to define the underlying mechanism for compound 20. We have added the following to the main text:

Discussion

"Recent work suggests that the ATP-competitive modulator GCN2iB can activate GCN2 independently of GCN1 under specific conditions using a GCN2 E26A mutant (9). In our hands, we did not observe GCN1-independent activation with GCN2iB at the concentrations tested. This discrepancy may reflect a narrow concentration window for GCN1-independent activation or context-dependent effects of the E26A mutation. These findings raise the possibility that GCN1-independent activation of GCN2 may occur under specific conditions or with distinct classes of compounds."

> *Strengths:*
>
> *Of the 3 compounds identified by the authors, C20 is the most interesting, not just for its intriguing mechanistic distinction as being GCN1-independent (shown genetically in two distinct cell lines, CHO and 293T in Figure 4, and in contrast to other GCN2 activators) but also for its potency. In in-cellulo assays, compound 21 appears as more of an ISR enhancer than an activator per se, and although compound 18 and compound 21 lead to upregulation of the ISR targets (Figure 2), that degree of upregulation is probably not significantly different from that induced by those compounds in Gcn2-/- cells. For C20, the effect appears stronger (although it is unclear whether the authors performed statistical analysis comparing the two genotypes in Figure 2D). In Figure 3, only C20 activates the ISR robustly in both CHO and 293T. Ultimately, C20 might be a tool for providing mechanistic insight into the details of GCN2 activation and regulation, and could be exploited therapeutically.*

Prompted by this suggestion, we assessed C20 in two additional commonly used cell lines: human colon carcinoma HCT116 cells and African green monkey COS7 cells. C20 showed no activity in these models. In contrast, primary mesothelioma cells (Mesobank T12) exhibited robust PPP1R15A induction in response to the compound. The following text has been added to the manuscript.

Results

"We went on to examine downstream cellular consequences of GCN2 activation in multiple models. While compounds did not induce detectable ISR signalling in HCT116 or COS-7 cells under the conditions tested, induction of PPP1R15A was observed in Mesobank T12 primary mesothelioma cells, indicating context-dependent biological responses… [data not shown]."

> *Weaknesses:*
>
> *There are some limitations to the existing work. As the authors acknowledge, they do not use any of the compounds in animals; their in vivo efficacy, toxicity, and pharmacokinetics are unknown. But even in the context of the in cellulo experiments, it is puzzling that none of the three compounds, including C20, has any effects in HeLa cells when Neratinib does. It's beyond the scope of this paper to address definitively why that is, but it would at least be reassuring to know that C20 activates the ISR in a wider range of cells, including ideally some primary, non-immortalized cells. In addition, the ISR is a complex, feedback-regulated response whose output varies depending on the time point examined. The in cellulo analysis in this paper is limited to reporter assays at 18 hours and qRT-PCR assays at 4 and 8 hours. A more extensive examination of the behaviour of the relevant ISR mRNAs and proteins (eIF2, ATF4, CHOP, cell viability, etc.) for C20 across*

> *a more extensive time course would give the reader a clearer sense of how this molecule affects ISR output.*

We thank the reviewer for this insightful suggestion. To address the need for a more comprehensive assessment of ISR signalling, we have extended our analysis across a broader time course and incorporated additional functional readouts. Using the ATF4-NanoLuc reporter, compounds 20 and 21 exhibit peak ISR activation at approximately 6-8 h in wild-type cells. In parallel, we assessed global mRNA translation using puromycin incorporation and found that compound 20, but not compound 21, induces a progressive reduction in translation over this period, which is dependent on GCN2. While we agree that direct measurement of upstream ISR markers such as eIF2α phosphorylation can be informative, detection of GCN2-mediated eIF2α phosphorylation is technically challenging and often less robust than activation of other ISR kinases (e.g. PERK). For this reason, we have prioritised orthogonal downstream functional readouts, including reporter activity and translational output, to capture ISR pathway engagement. These additional data provide a clearer picture of the kinetics and functional consequences of compound-induced ISR activation and have been incorporated into the revised manuscript.

Results

“Studies with compound 18 were limited by poor aqueous solubility; therefore, time-course analyses focused on compounds 20 and 21. To assess ISR activation over an extended period, live-cell luciferase measurements were performed using CHO cells stably expressing an ATF4::Nanoluc-PEST reporter. Both compounds elicited maximal reporter activation between 6 and 8 h (Figure S1A&B). Compound 20, but not 21, induced a significant GCN2-dependent reduction in mRNA translation, as measured by puromycin incorporation, with a progressive effect observed up to 7 h (Figure S1C-F).”

> *I also find it a bit strange that the authors describe C20 as "demonstrat(ing) weak inhibition of ... PKR" - the measured IC50 is ~4 μM, which is right around its EC50 for GCN2 activation. This raises the confounding possibility that C20 would simultaneously activate GCN2 while inhibiting PKR. While perhaps inhibition of PKR is not relevant under the conditions when GCN2 would be activated either experimentally or therapeutically, examining in cells the effects of C20 on GCN2 and PKR across a dose range would shed light on whether this cross-reactivity is likely to be of concern.*

We thank the reviewer for highlighting compound 20 as the most interesting lead compound and for recognising its apparent ability to activate GCN2 independently of GCN1. The reviewer identified several limitations relating to cell-type specificity, the temporal behaviour of ISR activation, and possible PKR cross-reactivity.

In response to the concern about cell-type specificity, we tested compound 20 in additional cellular models. Compound 20 did not induce detectable ISR signalling in HCT116 or COS-7 cells under the conditions tested, consistent with the reviewer’s observation that activity is not universal across cell types. However, we observed induction of PPP1R15A in primary Mesobank T12 mesothelioma cells. We have therefore revised the manuscript to present compound 20 activity as cell-context dependent rather than broadly generalisable across all cell types.

To address the reviewer’s concern that the ISR output was examined only at limited time points, we extended the time-course analysis for compounds 20 and 21. Using live-cell ATF4::NanoLuc reporter measurements, both compounds showed maximal reporter activation at approximately 6-8 hours. We also measured translational output by puromycin incorporation and found that compound 20, but not compound 21, caused a progressive GCN2-dependent reduction in translation. These data provide a clearer view of the kinetics and functional consequences of compound 20-mediated ISR activation.

The reviewer also noted that compound 20 inhibits PKR *in vitro* at concentrations close to those required for GCN2 activation in cells. We agree that this is an important potential liability. Because PKR signalling was not robustly or reproducibly inducible in our CHO-based reporter system, we were unable to perform a reliable cellular dose-response analysis of PKR engagement in the present study. We have therefore revised the Discussion to acknowledge kinase cross-reactivity, including possible PKR inhibition, as an important limitation and an issue for future development of this chemical series.

Finally, we have moderated our mechanistic interpretation of compound 20. Although the data support direct engagement of GCN2 and suggest a mechanism distinct from canonical GCN1-dependent activation, we now discuss GCN1-independent activation more cautiously and in the context of prior reports that GCN2iB can display GCN1-independent activity under specific experimental conditions.

Discussion

"While the functional relevance of PKR inhibition in our cellular systems is uncertain, these observations highlight the potential for kinase cross-reactivity, which will be important to address in future studies."

> ***Recommendations for the authors:***
>
> ***Reviewer #1 (Recommendations for the authors):***
>
> *(1) The description of the chemical screen for Gcn2 activators is not sufficiently clear and detailed. a) Briefly and early on provide the rationales (modes of action) for using histindinol and latruculin A. Explain further the rationale in Figure 2, outlining the purpose for the combined compound + submaximal dose of histindinol.*

The text has been amended.

Results

"Histidinol activates GCN2 by inhibiting histidyl-tRNA synthetase, leading to the accumulation of uncharged tRNAHis. This uncharged tRNA binds to GCN2, relieving its autoinhibition and activating the kinase (35). Latrunculin A sequesters G-actin, thereby inhibiting PPP1R15A activity (36, 37). Tunicamycin inhibits protein glycosylation in the endoplasmic reticulum (ER), resulting in activation of PERK (38)."

"This submaximal concentration was used to allow detection of compounds that enhance ISR signalling when GCN2 is partially activated."

> *b) What is unique about the second CHO: ATF4-luc2 reporter line? Why do only 89 out of the original 130 compounds induce the ISR in this line versus the original CHO: ATF4-Nanoluc cell line? This is confusing for the reader about how compounds were triaged for characterization.*

The ATF4-Nanoluc and ATF4-luc2 reporter lines differ only in the luciferase used, but this has important practical consequences. The Nanoluc reporter is substantially more sensitive, so it was used for the primary screen to detect even weak ISR activation. The luc2 reporter has lower sensitivity and a narrower dynamic range, making it a more stringent orthogonal assay. As a result, not all hits from the Nanoluc screen (130 compounds) reproduced in the luc2 line; the 89 compounds retained are those that robustly activate the ISR under these more stringent conditions. This step was therefore used to prioritise stronger, more reproducible activators for downstream characterisation.

Results

"While primary screening was performed in ATF4-Nanoluc lines for maximal sensitivity, hits were subsequently re-tested in a second CHO ATF4::luc2 reporter line as a more stringent orthogonal assay to prioritise robust ISR activators. Of the 130 hits identified in the sensitive Nanoluc screen and passing early toxicity assessment, 89 were confirmed in the luc2 assay, consistent with enrichment for higher-amplitude ISR activators under more stringent detection conditions."

> *c) The study uses a second CHO reporter line in the flow scheme (CHO:ATF4-luc2) and then switches back to an ATF4-Nanoluc line to establish GCN2 dependence. What is the rationale for switching back to the original reporter line?*

The luc2 reporter line was used as a more stringent, orthogonal validation step to prioritise robust ISR activators. For subsequent mechanistic studies, including assessment of GCN2 dependence, we returned to the ATF4-Nanoluc line because its higher sensitivity and simpler single-reagent assay format are better suited to multi-point measurements and comparative analyses. In effect, the luc2 reporter was used for triage, whereas the Nanoluc system was retained for mechanistic characterisation and downstream screening.

Results

"In subsequent mechanistic studies, the ATF4-Nanoluc reporter was again used to take advantage of its higher sensitivity and simpler assay format for multi-condition comparisons."

> *d) The rationale for the first orthogonal screen described in the results section to identify inducers of ER stress is not clearly explained. The compounds were already determined to be dependent on GCN2 prior to this test, and one would have thought that this criterion would have covered ER stress and alternative eIF2 kinase activators.*

We agree with the reviewer that, in principle, establishing GCN2 dependence should reduce the likelihood of capturing compounds acting through alternative eIF2α kinases. However, we performed this orthogonal ER stress screen to address two practical considerations. First, high-throughput screening is inherently prone to false positives, as it is typically conducted at a single concentration and time point, and compound libraries may contain degraded or chemically inconsistent material. We therefore used a lower-throughput, more controlled ER stress assay with freshly sourced compounds and additional readouts (e.g. CHOP and XBP1) to improve confidence in the hits. Second, despite prior evidence of GCN2 dependence, ER stress signalling via PERK converges on the same downstream endpoints: eIF2α phosphorylation and ATF4 induction. We therefore wished to explicitly exclude compounds that activate the ISR indirectly via ER stress. In practice, this proved important, as the orthogonal assay did identify compounds that induced ER stress, which we subsequently excluded from the lead set.

Results

"Although hits were prioritised for GCN2 dependence, we performed an additional orthogonal screen to exclude compounds that activate the ISR indirectly via ER stress, which converges on the same downstream outputs."

> *(2) A major point of the manuscript is that there is GCN1 independence for the small molecule activation of GCN2, and this has not yet been reported. One report for this GCN1 independence is reference 9 [Carlson … Wek 2023] (Figure 5). In this report, low doses of GCN2iB that can activate GCN2 (although by the present manuscript at much lower levels than the identified new compounds) induce ATF4 expression in cells expressing an E26A mutant of GCN2 that is suggested to negate GCN1 binding and*

> *enhancement of GCN2 activity. Halofuginone induction of ATF4 expression was thwarted by the GCN2 E26A mutant.*

We thank the reviewer for highlighting this important point. We agree that Carlson et al. (2023) suggest that, under certain conditions, GCN2iB can activate GCN2 independently of GCN1 using the E26A mutant. In our experiments, however, we did not observe GCN1-independent activation with GCN2iB under the conditions tested, i.e. similar low doses. One possible explanation is that the GCN1-independent activity reported by Carlson et al. occurs only within a narrow concentration range; their observations were made at very low compound concentrations, whereas higher concentrations may engage additional regulatory mechanisms. In our study, we used concentrations optimised for robust ISR activation, which may mask such effects. We also note that the E26A mutation (E18A in yeast), originally identified by two-hybrid analysis, disrupts the GCN2-GCN1 interaction but may not completely eliminate all modes of functional coupling under all conditions. Taken together, these observations raise the possibility that GCN1-independent activation represents a context-dependent mechanism that may be unmasked only under specific experimental conditions or by particular classes of compounds.

We have revised the Discussion to acknowledge this prior report explicitly and to clarify how our findings relate to it.

Discussion

“Recent work suggests that the ATP-competitive modulator GCN2iB can activate GCN2 independently of GCN1 under specific conditions using a GCN2 E26A mutant (9). In our hands, we did not observe GCN1-independent activation with GCN2iB at the concentrations tested. This discrepancy may reflect a narrow concentration window for GCN1-independent activation or context-dependent effects of the E26A mutation. These findings raise the possibility that GCN1-independent activation of GCN2 may occur under specific conditions or with distinct classes of compounds.”

> *(3) The authors state that the ISR was exaggerated in Ppp1r15a KO cells. It would be helpful to include statistical analyses to support this statement.*

Thank you for enabling us to be more precise. New text added:

Results

“Activation of the ISR by tunicamycin was exaggerated in the *Ppp1r15a*$^{-/-}$ cells owing to their defective dephosphorylation of eIF2a (wild type vs *Ppp1r15a*$^{-/-}$, $p<0.05$).”

> *(4) The results state that Chop and Ppp1r15a mRNAs were measured following 4 hours of treatment with compound 18, 20, or 21, but Figure 2D shows treatment from 0 to 8 hours? It appears that the compound still induces these mRNAs in GCN2 KO cells, possibly with delayed kinetics. A lengthened time course study would help determine if this is indeed the case.*

We thank the reviewer for this careful observation. To address the reviewer’s point regarding delayed or GCN2-independent signalling, we have extended our analysis using compounds 20 and 21, which are more tractable experimentally (solubility). Using the ATF4-Nanoluc reporter, both compounds show peak ISR activation at ~6–8 h in wild-type cells over an extended time course. In parallel, functional readouts of mRNA translation (puromycin incorporation) demonstrate that compound 20, but not 21, induces a progressive, GCN2-dependent reduction in translation over this period. These clarify the temporal aspects of signalling by these two compounds.

Results

“Studies with compound 18 were limited by poor aqueous solubility; therefore, time-course analyses focused on compounds 20 and 21. To assess ISR activation over an extended period, live-cell luciferase measurements were performed using CHO cells stably expressing an ATF4::Nanoluc-PEST reporter. Both compounds elicited maximal reporter activation between 6 and 8 h (Figure S1A&B). Compound 20, but not 21, induced a significant GCN2-dependent reduction in mRNA translation, as measured by puromycin incorporation, with a progressive effect observed up to 7 h (Figure S1C-F).”

Legend

“Supplementary Figure S1. Kinetics of responses to compounds 20 and 21

(A-B) Wild-type CHO cells stably expressing the ATF4::nanoLuc-PEST reporter were treated with Nano-Glo and either (A) 13mM compound 20 or (B) 13mM compound 21. Median bioluminescence (fold change normalised to DMSO control) ± 95% confidence. Representative experiment (n=4 technical repeats). (C-F) Representative immunoblot of lysates from wild-type or *Eif2ak4*$^{-/-}$ CHO cells treated with 10μM compound 20 or 7.5μM 21 for the indicated times. Immediately before harvesting, cells were treated with 10μg/mL puromycin to label newly synthesised polypeptides. “-“ indicates cells not incubated with puromycin. “U” cells were treated with puromycin but without test compound. “CHX” represents the cycloheximide control (100μg/mL). Molecular size in kDa. (E-F) Quantification of puromycinylated proteins normalised to GAPDH. Mean ± SEM. CHO WT (black) and *Eif2ak4*$^{-/-}$ cells (turquoise. N = 4 independent experiments. Two-way ANOVA with Šídák's multiple comparisons test; ***: $p \leq 0.001$.”

> *(5) In the section describing the differences between cell lines in the ability of compounds to induce the ISR, this is difficult for the reader to interpret, as no controls are included. How does histidinol (or other canonical inducers of the ISR) behave in the three reporter assays (CHO, 293T, and HeLa)?*

As requested, we now provide ATF4::Nanoluc reporter activation (3mM, 20 hours because of this drug’s slow kinetics)

Results

“To benchmark ISR activation in these models, each cell type was treated with 3mM histidinol (Figure S2). Reporter activation was most robust in CHO cells, followed by 293T cells, then HeLa cells.”

Discussion

“Moreover, histidinol-induced ISR activation showed a clear hierarchy across cell lines, with CHO cells being the most responsive and HeLa cells the least.”

Legend

“Supplementary Figure S2. Cell-type differences in response to histidinol

Fold-change of ATF4::NanoLuc reporter signal in HEK293T, HeLa and CHO cells transiently transfected with reporter and treated for 20 hours with 3mM histidinol. Fold-change calculated relative to vehicle control. Mean ± SEM).”

We thank the reviewer for this important question. However, we respectfully disagree that a direct correspondence between the concentrations required for target engagement in the BRET assay and for ISR activation in functional assays should necessarily be expected. BRET (including NanoBRET) is a target engagement assay that measures compound binding to the protein in intact cells, typically by competition with a labelled tracer, and thus reports on

apparent intracellular affinity and occupancy rather than downstream biological effect (Robers 2019, PMID 30519940). By contrast, ISR activation is a functional readout that reflects amplification through signalling networks, and can be influenced by multiple additional variables including pathway non-linearity, feedback, and kinase regulation. Consequently, it is well established that potencies derived from target engagement assays do not always align with those measured in functional assays. For example, intracellular kinase profiling studies using NanoBRET have demonstrated systematic potency offsets between binding/engagement measurements and downstream cellular activity, arising from factors such as intracellular ATP competition and pathway context (PMID Capener 2026, PMID 41495225). More generally, target engagement assays provide a quantitative measure of binding, whereas functional assays measure biological outcome, and these readouts need not coincide because they capture distinct aspects of a compound's mechanism of action. Accordingly, we interpret our BRET data as evidence of direct interaction with GCN2 in cells, rather than as a predictor of the concentration required to activate the ISR. The observation that higher concentrations are required in the BRET assay is therefore not unexpected and does not argue against a requirement for kinase-domain engagement in ISR activation. Instead, it reflects the different mechanistic endpoints captured by the two assay formats.

We will clarify this point explicitly in the revised manuscript.

Results

"The concentrations required to detect target engagement in NanoBRET assays did not directly mirror those required for ISR activation, reflecting the distinction between ligand binding and downstream pathway output."

> *(7) In Figure 5E, the authors suggest that compounds 18 and 20 are non-competitive inhibitors of GCN2 since the Vmax increases with increasing ATP concentration. What is the Km for ATP in the absence or presence of compound 18 or 20? It would be helpful to include progress curves as supplementary data to support the Vmax plots in Fig. 5E. Consider providing more specific units (currently arbitrary units) for the y-axis.*

We thank the reviewer for this insightful comment and agree that our original wording overstated the mechanistic interpretation of these data. In particular, the use of the term "non-competitive" is not well supported by the current analysis and may be misleading, especially given that our data are consistent with binding within or proximal to the ATP-binding pocket. We have therefore revised the text to remove this designation and instead describe the data more conservatively in terms of changes in apparent Vmax, without assigning a specific inhibition mechanism. With respect to kinetic analysis, we agree that full determination of K^m values and inclusion of progress curves would provide a more rigorous mechanistic interpretation. However, given the primary focus of this manuscript on identifying and characterising small-molecule activators of GCN2 in cells, we believe that a detailed steady-state kinetic analysis would be beyond the scope of the current study. We have therefore moderated our conclusions accordingly and now present these data as preliminary kinetic observations rather than definitive evidence of inhibition modality.

Results

"Compounds 18 and 20 altered the apparent kinetic parameters of GCN2, including an increase in the observed V_{max}; however, these data do not allow assignment of a specific inhibition modality."

> *(8) The full-length GCN2 assay presented in Figure 5G appears to be unresponsive to uncharged tRNA, a known regulator of GCN2. The statement that compound 20 induces eIF2 phosphorylation to a greater extent than tRNAs is true for the in vitro assay, but arguably is because the in vitro assays do not recapitulate the in vivo arrangement.*

We thank the reviewer for this comment. We respectfully disagree that the assay is unresponsive to uncharged tRNA. In our hands, GCN2 does exhibit activation in response to tRNA; however, the magnitude of this effect is modest (~4-fold) compared to the substantially stronger activation observed with compound 20 (~40-fold). As a result, the tRNA response can appear compressed when both are plotted on the same scale. We agree with the reviewer that the in vitro assay does not fully recapitulate the in vivo regulatory environment, where factors such as GCN1 and ribosome association are known to potentiate GCN2 activation. This limitation likely explains the relatively weaker response to tRNA under our assay conditions and was a key motivation for incorporating cellular assays in our study. Interestingly, the marked difference in activation magnitude between tRNA and compound 20 in vitro raises the possibility that compound-mediated activation may, at least in part, bypass regulatory features that normally constrain GCN2 activity in a GCN1-dependent manner. While we have not directly tested this hypothesis, we will temper the wording and include this as a speculative point in the Discussion.

Results

"Of note, uncharged tRNA produced a modest (~4-fold) activation of GCN2 under these conditions, whereas compound 20 induced substantially greater (~40-fold) activation."

Discussion

"The markedly greater activation observed with compound 20 compared with uncharged tRNA in vitro raises the possibility that such compounds may partially bypass regulatory constraints on GCN2 activation, including those normally mediated by GCN1."

> *(9) Using purified GCN2 kinase domain at low ATP concentrations (10 μM), compounds 18 and 20 were shown not to inhibit GCN2 up to concentrations of 3 μM. In previous assays, much higher concentrations of compounds 18 and 20 were used to inhibit GCN2. Why were different concentrations used? This makes this interpretation of this data difficult for the reader to draw conclusions.*

We thank the reviewer for this comment and agree that the use of different concentration ranges across assays may not have been sufficiently clear. The kinase-domain assay performed at low ATP (10 μM) was specifically designed to assess whether compounds 18 and 20 have a propensity to inhibit GCN2 under conditions that sensitise detection of ATP-competitive effects and facilitate comparison with related eIF2α kinases. This assay was therefore optimised for detecting inhibition, rather than activation. In contrast, the higher concentrations used in other experiments were selected to robustly measure ISR activation in cellular or full-length protein contexts, where higher compound exposure is required to observe downstream signalling outputs. These two assay systems therefore address distinct mechanistic questions—targeting inhibition under controlled biochemical conditions versus activation in more complex functional settings—and are not directly comparable in terms of concentration–response relationships. We will revise the manuscript to clarify this distinction and to emphasise that the kinase-domain assay was not intended to define the activation potency of the compounds.

Results

"This assay was performed at low ATP concentrations to sensitise detection of ATP-competitive inhibition and was not optimised to detect compound-mediated activation of GCN2."

> *(10) In silico docking studies support the binding of compound 20 in the ATP-binding pocket of the GCN2 kinase domain. How is this compatible with the stated ATP non-competitive mechanism?*

We agree with the reviewer that our previous description was misleading. The designation of compounds 18 and 20 as "ATP non-competitive" is not supported by the available data and is inconsistent with the docking results suggesting binding within the ATP-binding pocket. We have therefore revised the manuscript to remove this terminology and to describe the kinetic behaviour more cautiously, without assigning a specific mode of inhibition.

> *(11) The study does not appear to feature biological assays demonstrating the effects of GCN2 activation. For example, does compound 20 reduce translation or growth of cells in a GCN1/GCN2-dependent manner, or do the compounds overcome PVOD mutations akin to the authors' Hum Mol Genet 2024 Aug 18;33(17):1495-1505 article?*

We thank the reviewer for this suggestion. We agree that defining downstream biological consequences of GCN2 activation is an important goal. We did explore this using several cellular systems; however, these effects were context-dependent and not consistently observed across models. Specifically, compounds did not induce a detectable ISR in HCT116 or COS-7 cells under the conditions tested, despite responsiveness of these systems to canonical activators such as histidinol. In contrast, we did observe induction of PPP1R15A in primary mesothelioma cells, indicating that biological responses can be elicited in certain cellular contexts. We also tested whether these compounds could rescue disease-associated GCN2 variants linked to PVOD, as previously reported for GCN2iB, but did not observe activation of these mutants. These findings suggest that while the compounds robustly activate GCN2 signalling in reporter assays, downstream biological outputs are context-dependent and may require specific cellular conditions or co-factors. Given the variability across systems, we have limited our conclusions to ISR activation and have not generalised broader biological effects. We will clarify this point in the revised manuscript.

Results

"We went on to examine downstream cellular consequences of GCN2 activation in multiple models. While compounds did not induce detectable ISR signalling in HCT116 or COS-7 cells under the conditions tested, induction of PPP1R15A was observed in Mesobank T12 primary mesothelioma cells, indicating context-dependent biological responses. Moreover, in contrast to GCN2iB (17), the current compounds did not activate disease-associated GCN2 variants linked to PVOD [data not shown]."

> *(12) For the control of neratinib and other activators linked with ATP binding that are suggested to be dependent on GCN1 in Fig. 4, include reporter induction by drug treatment in Gcn2-/- cells. It would be helpful to be clear in the list of compounds between those suggested to be direct activators versus those that may create stress that leads to GCN2 activation.*

We thank the reviewer for this suggestion. In response, we have performed additional reporter assays in both WT and *GCN2*$^{-}$/- cells to assess the dependence of drug-induced ISR activation on GCN2. These experiments reveal clear GCN2 dependence for reporter induction upon treatment with sunitinib, NXP800, WEE1-in-4, Debio0123, gefitinib, and erlotinib, as signal is markedly reduced in GCN2$^{-/-}$ cells compared to WT.

In contrast, dovitinib and AZD1775 show less clear dependence, with relatively low reporter signal even in WT cells (notably lower than observed in Fig. 4C), limiting interpretation. Interestingly, dabrafenib induces stronger reporter activity in GCN2$^{-/-}$ cells than in WT, indicating that its effects are independent of GCN2 and may reflect activation of alternative stress or signalling pathways.

Results

“To further assess the mechanism of compound-induced ISR activation, we evaluated reporter responses in GCN2-deleted cells (Supplementary Figure S3). Several compounds, including sunitinib, NXP800, WEE1-in-4, Debio0123, gefitinib, and erlotinib, showed reduced reporter activity in GCN2-deficient cells, consistent with GCN2-dependent activation. In contrast, dovitinib, AZD1775 and dabrafenib produced weaker or inconclusive responses even in the paired wild-type lines, limiting analysis. These data allow us to distinguish compounds consistent with direct or GCN2-dependent activation from those more likely to induce ISR indirectly through cellular stress upstream of GCN2. These findings support a distinction between compounds that activate the ISR through GCN2-dependent mechanisms and those that likely act indirectly via alternative stress pathways.”

Legend

“Supplementary Figure S3. GCN2-dependence of ISR activation by putative GCN2 agonists

Normalised fold-change in ATF4 signal in CHO WT (purple) and Gcn2-/- (blue) ATF4::NanoLuc reporter cells treated for 19 hours with a panel of ATP-competitive kinase inhibitors reported to activate GCN2 (at 1 and 3μM, sunitinib used at 3 and 10μM, AZD1175 used at 0.3 and 1μM, gefitinib and erlotinib used at 3 and 10μM). DMSO was used as vehicle control. (n=3; mean ± SEM).”

> *Minor Comments:*
>
> *(1) In the introduction, the authors state that "Several type 1 and 1.5 kinase inhibitors can activate GCN2 at low concentrations while inhibiting at higher concentrations". What is the evidence that type I inhibitors can activate GCN2?*

Thank you for this query. We believe our initial phrasing was open to misinterpretation. The new wording is

Introduction

“Several kinase inhibitors classified as type 1 or type 1.5 with respect to their canonical targets can activate GCN2 at low concentrations while inhibiting it at higher concentrations; however, their binding mode to GCN2 remains undefined.”

> *(2) A CHO:ATF4-Nanoluc translation reporter screen was used to screen 123K compounds and divide them into a pool of inhibitors and a pool of activators. The criteria used to make this distinction are not sufficiently described in the manuscript, and screen results are not supplied as supplementary data.*

We thank the reviewer for highlighting the need for greater clarity regarding the screening criteria and reproducibility. Compounds from the primary screen (BioAscent library of 123,222 drug-like compounds performed by the ALBORADA Drug Discovery Institute) were classified based on Z-score thresholds, with activators defined as those with Z-score > 3. To assess robustness, the primary screen data were re-analysed independently. In an initial analysis of 121,000 compounds (excluding plates failing quality control), 6,521 compounds met the activator threshold. Of these, 6,461 overlapped with the original hit list. The small number of discrepancies included: (i) compounds absent from the analysed dataset (e.g. originating from failed plates), and (ii) compounds with Z-scores close to the threshold (typically between −3 and −3.02), consistent with minor analytical variation (e.g. rounding). Overall, these analyses show a high degree of concordance in hit identification, with differences restricted to borderline cases near the selection threshold. We have clarified these criteria below.

Results

“Compounds were classified based on Z-score thresholds derived from the primary screen, with activators defined as those with Z-score > 3. An initial analysis of 121,000 compounds, excluding plates failing quality control, identified 6,521 activators, of which 6,461 overlapped with the subset selected for follow-up screening. Minor discrepancies were restricted to compounds absent from the analysed dataset (e.g. originating from failed plates) or those with Z-scores close to the threshold (3 to 3.02), consistent with limited analytical variation. Using this approach, we assembled a subset of 6,461 compounds enriched for potential ISR activators and screened these in 384-well format at 10 μM for 16 hours.”

> ***Reviewer #3 (Recommendations for the authors):***
>
> *(1) The legend to Figure 4 should read "Compound 20 displays GCN1 independence", not "dependence".*

Thank you for spotting this error. We have made the correction.

> *(2) The text describes Figure 2D as examining 4h, but it also examines 8h.*

We have amended the text to:

“After validating their effects using the assays described above, we next confirmed activation of the ISR by these compounds at the transcriptional level at 4 and 8 hours.”

> *(3) Unless I'm misreading Table S1, compound Z134826202 is listed as activating the ISR, but the authors describe it in the text as inactive.*

Thank you. We have corrected this error.

https://doi.org/10.7554/eLife.108590.2.sa0